USGS
science for a changing world

Prepared for the National Aeronautics and Space Administration

Geologic Map of the Northern Plains of Mars

By Kenneth L. Tanaka, James A. Skinner, Jr., and Trent M. Hare

Pamphlet to accompany
Scientific Investigations Map 2888

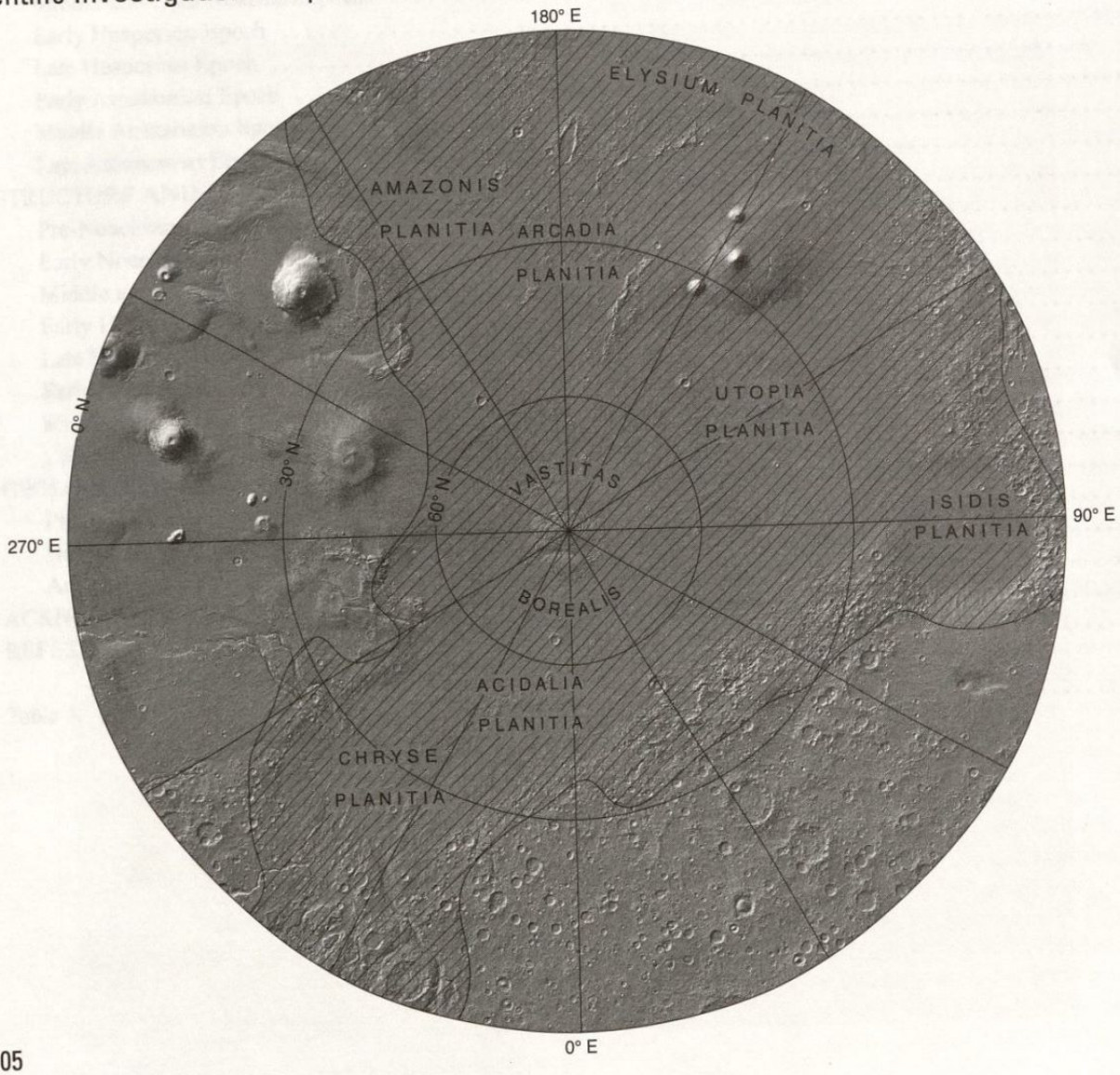

2005

U.S. Department of the Interior
U.S. Geological Survey

CONTENTS

INTRODUCTION

The northern plains of Mars cover nearly a third of the planet and constitute the planet's broadest region of lowlands. Apparently formed early in Mars' history, the northern lowlands served as a repository both for sediments shed from the adjacent ancient highlands and for volcanic flows and deposits from sources within and near the lowlands. Geomorphic evidence for extensive tectonic deformation and reworking of surface materials through release of volatiles occurs throughout the northern plains. In the polar region, Planum Boreum contains evidence for the accumulation of ice and dust, and surrounding dune fields suggest widespread aeolian transport and erosion.

The most recent regional- and global-scale maps describing the geology of the northern plains are largely based on Viking Orbiter image data (Dial, 1984; Witbeck and Underwood, 1984; Scott and Tanaka, 1986; Greeley and Guest, 1987; Tanaka and Scott, 1987; Tanaka and others, 1992a; Rotto and Tanaka, 1995; Crumpler and others, 2001; McGill, 2002). These maps reveal highland, plains, volcanic, and polar units based on morphologic character, albedo, and relative ages using local stratigraphic relations and crater counts.

This geologic map of the northern plains is the first published map that covers a significant part of Mars using topography and image data from both the Mars Global Surveyor and Mars Odyssey missions. The new data provide a fresh perspective on the geology of the region that reveals many previously unrecognizable units, features, and temporal relations. In addition, we adapted and instituted terrestrial mapping methods and stratigraphic conventions that we think result in a clearer and more objective map. We focus on mapping with the intent of reconstructing the history of geologic activity within the northern plains, including deposition, volcanism, erosion, tectonism, impact cratering, and other processes with the aid of comprehensive crater-density determinations. Mapped areas include all plains regions within the northern hemisphere of Mars, as well as an approximately 300-km-wide strip of cratered highland and volcanic regions, which border the plains. Note that not all of the contiguous northern plains are mapped, because some minor parts of Elysium and Amazonis Planitiae lie south of the equator.

PHYSIOGRAPHIC SETTING

The northern plains of Mars are broadly characterized by a smooth, gently sloping surface (Kreslavsky and Head, 2000) that covers much of the planet's northern hemisphere below the mean planetary radius (fig. 1). We delineate three distinct regional topographic basins (fig. 1), informally named Borealis basin (encompassing the polar region), Utopia basin, and Isidis basin. Collectively, the basin floors generally range in elevation from –3,000 to –5,000 m. The plains are bounded to the south by densely cratered highland terrains and by the broad informally named Tharsis rise (fig. 1), which includes the Olympus Mons and Alba Patera shield volcanoes, as well as the arcuate, broad ridge cut by Acheron Fossae and the grooved aureole of Olympus Mons (Lycus Sulci). The informally named Elysium rise (fig. 1), which includes the Elysium Mons, Hecates Tholus, and Albor Tholus volcanoes, is the largest volcanic province that occurs entirely within the lowlands. Southeast of the Elysium rise, Elysium Planitia connects to Arcadia and Amazonis Planitiae between the Elysium and Tharsis rises. Acidalia and Chryse Planitiae form an embayment between Tempe and Arabia Terrae. Syrtis Major Planum consists of a broad shield west of Isidis Planitia, whereas Lunae Planum is a high plain in the eastern part of the Tharsis rise. The rugged peaks of Libya Montes ring the south margin of Isidis Planitia.

Systems of ridges, troughs, fractures, and channels and dispersed craters mark the northern plains. The largest mountainous region in the northern plains is the north-trending, degraded ridges of Phlegra Montes located northeast of the Elysium rise. Gordii and Eumenides Dorsa form broad ridges that extend from the Tharsis rise into Amazonis Planitia. Tantalus Fossae are narrow, linear, and shallow troughs that extend to the northeast from the Alba Patera shield volcano into adjacent plains. Similarly, Elysium Fossae form deep, curvilinear, irregular troughs mainly on the northwest flank of the Elysium rise. A system of deep, wide outflow channels (Kasei, Maja, Shalbatana, Simud, Tiu, Ares, and Mawrth Valles) emanate from chaotic terrains within Xanthe and Margaritifer Terrae, incise the highland plateau, and extend into Chryse Planitia. Other channel features extend from Elysium Fossae (Hrad, Granicus, Apsus, and Tinjar Valles) to the northwest into the central part of Utopia basin. Hephaestus Fossae and Hebrus Valles are unusual drainage systems that consist of polygonal troughs, collapse depressions, and channels in southeastern Utopia Planitia. Amenthes Cavi* form a band of arcuate depressions within southern Utopia Planitia. On the southeast flank of the Elysium rise, the curvilinear fractures of Cerberus Fossae appear to be the source of Athabasca and Grjotá* Valles. These channel features, along with Rahway Valles*, extend from the southeast margin of the Elysium rise into Elysium Planitia. Marte Vallis forms a broad channel connecting Elysium and Amazonis Planitiae to the east. Networks of polygonal troughs disturb the plains surface at Adamas Labyrinthus in Utopia Planitia and at Cydonia Labyrinthus in southeastern Acidalia Planitia. Many large craters occur within the northern plains, including the double-ring Lyot crater near Deu-

*Provisionally approved by International Astronomical Union

teronilus Mensae and the elliptical Orcus Patera along the northeast margin of Elysium Planitia.

In general, the highland/lowland boundary (highland not mapped) is fragmented into large mesas and knobs, including Nepenthes, Deuteronilus, Protonilus, and Cydonia Mensae and Tartarus Montes and their surrounding detrital plains. Within northern Acidalia Planitia, Acidalia Mensa forms a large mesa adjoined by Acidalia Colles, an area of knobs formed within a shallow depression. Other patches of knobs and knobby mountain ranges in the plains include Scandia Colles north of Alba Patera, Galaxias Colles north of the Elysium rise, Tartarus Colles and Tartarus and Erebus Montes in and near Arcadia Planitia, Ortygia Colles east of Acidalia Colles, and Astapus Colles in western Utopia Planitia. Irregular depressions are associated with many of the knobby terrains.

Planum Boreum forms a 1- to 2-km-high, 1,000-km-diameter north polar plateau marked by a series of troughs, Borealis and Gemini Scopuli*, as well as by Chasma Boreale, a 100-km-wide and 1.5-km-deep chasm marked by two isolated depressions approximately 50 km wide, Boreum and Tenuis Cavi*. West of Chasma Boreale, the base of Planum Boreum is marked by an irregular scarp, Rupes Tenuis, that reaches as much as 1,000 m in height. Between Planum Boreum and Scandia Colles, irregular depressions form Scandia Cavi, while low, circular, irregular domes form Scandia Tholi. Dune fields surrounding the planum include Olympia, Abalos, and Hyperboreae Undae.

DATA

The base map image is derived from the Mars Orbiter Laser Altimeter (MOLA) instrument onboard the National Aeronautics and Space Administration (NASA) Mars Global Surveyor (MGS) spacecraft (Albee and others, 2001; Smith and others, 1999, 2001). The image represents a few hundred million measurements gathered between 1999 and 2001 (Neumann and others, 2001). The measurements were converted into a digital elevation model (DEM; Neumann and others, 2001; Smith and others, 2001) with a resolution of 128 pixels/degree. In projection, the pixels are 463.086 m in size at the equator. Data are sparse near the pole (above lat 87° N.), because the area was sampled by off-nadir altimetry tracks. Gaps between tracks of 1–2 km are common, and some gaps of as much as 12 km occur near the equator. DEM points located in these gaps in MOLA data were filled by interpolation.

The polar stereographic projection is used for the hemispheric base and encompasses lat 0° to 90° N. with a central meridian of lat 0° N. The adopted equatorial radius is 3,396.19 km (Seidelmann and others, 2002). Longitude increases to the east and latitude is planetocentric as allowed by IAU/IAG (International Astronomical Union/International Association of Geodesy; Seidelmann and others, 2002) standards and in accordance with current NASA and U.S. Geological Survey (USGS) standards. A secondary grid (printed in red) has been added to the map as a reference to the west longitude/planetographic latitude system that is also allowed by IAU/IAG standards (Seidelmann and others, 2002) and has historically been used for Mars. Calculation of the planetographic grid is based on an oblate spheroid with an equatorial radius of 3,396.19 km and a polar radius of 3,376.2 km (Seidelmann and others, 2002).

To create the topographic base image, the original DEM produced in simple cylindrical projection with a resolution of 128 pixels/degree was projected into the polar stereographic projection of the hemispheric base. This was mosaicked with another DEM produced in polar stereographic projection that covered lat 70° to 90° N. A shaded-relief base was generated from the combined DEM with a sun angle of 45° from horizontal and a sun azimuth of 225° (northwest), measured clockwise from north, and a vertical exaggeration of 100 percent (the illumination algorithm assumes a planar, Cartesian surface). The file was then scaled to 1:15,000,000 at the north pole with a resolution of 300 dots/inch.

Geographic names are shown for features clearly visible at the scale of this map. Names are adopted by the IAU, except for those denoted with an asterisk (*), which are provisionally approved. For a complete list of IAU-approved nomenclature for Mars, see the Gazetteer of Planetary Nomenclature at http://planetarynames.wr.usgs.gov.

Our primary mapping dataset was the MOLA DEM at 128 pixels/degree. Because of increasing data density poleward, the lower latitude between-track (east-west) spacing can locally exceed several kilometers, resulting in interpolated elevation points. However, above approximately lat 60° N. and lat 78° N., altimetry data-point spacing permitted the construction of higher resolution DEMs (respectively, 256 pixels/degree or ~230 m/pixel and 512 pixels/degree or 115 m/pixel). We generated and relied on numerous derived MOLA products to assist in geologic mapping and characterization, including cell-to-cell slope, aspect (slope direction), local contour, and color shaded-relief maps. Similar to the detrended MOLA maps used by Head and others (2002), we ran a 75-km bounding-box median high-pass filter (MHPF) on the DEM to remove (or detrend) the regional surface slope and enhance local relief. Slope maps helped us to characterize surface texture and landforms while the MHPF DEM helped us to trace subtle landforms and geologic boundaries.

We also used the Viking Orbiter Mars Digital Image Mosaic version 2.0, which provided both morphologic and albedo information at as much as 1/256° resolution (~230 m/pixel), as well as Mars Orbiter Camera (MOC)

wide-angle images (~250 m/pixel) acquired by MGS. These data were particularly helpful in mapping low-latitude regions where MOLA tracks are widely spaced, and the polar residual ice was identified from albedo. Though MGS MOC narrow-angle images (>1.4 m/pixel) are too dispersed to use for geologic mapping, they proved very useful for unit identification where diagnostic morphologic features could be identified. Finally, we used available Mars Odyssey (MO) Thermal Emission Imaging System (THEMIS) images, consisting of infrared (100 m/pixel, daytime and nighttime) and visible (17–40 m/pixel, 1 to 5 spectral bands) types, to locate subtle contacts difficult to follow in either MOLA DEM or Viking or MOC wide-angle images. The THEMIS daytime infrared and visible images commonly reveal detailed morphologic character not apparent in Viking images. At middle and lower latitudes, THEMIS daytime and nighttime infrared images displayed contrasts in thermophysical properties of surface materials that, in some cases, assisted in differentiating geologic units.

METHODOLOGY

We implement comprehensive geologic mapping methods that differ in many respects from previous approaches common to planetary geologic mapping, with the goal of achieving a clearer and more objective product. Our methodology involves carefully considered schemes for (1) delineating, naming, grouping, and symbolizing map units, (2) coloring units by age, (3) identifying contact types, and (4) mapping geomorphic features. Our mapping was facilitated and enhanced by using Geographic Information Systems (GIS) software mapping tools.

UNIT DELINEATION

Consistent with the approach that Hansen (2000) applied to Venus mapping, we identify and map rock units and sedimentary cover on the basis of their apparent geologic uniqueness as defined by their primary physical features, areal extent, relative age, and geologic associations. Primary features, including lobate flow scarps, layering, albedo, and thermophysical character, formed during emplacement; whereas secondary features, including fault scarps, yardangs, valley networks, and wind streaks, are formed after emplacement. In many cases, delineating primary and secondary features requires careful observation and may be difficult and uncertain where overprinting of secondary features has masked, obliterated, or mixed with primary features.

Map units require sufficient areal extent and geologic significance to be effectively portrayed at map scale and to reduce the clutter that mapping smaller ones imposes. We chose areas approximately 50 km across for the smallest mapped noncrater units and approximately 100 km across for the smallest mapped crater units. Thus, small local outcrops of what may be unique geologic materials are included in more extensive units. Where extensive outcrops are too small to map, they become part of composite units; for example, small knobs and mesas of the Noachis Terra unit along the highland/lowland boundary are included with adjacent plains-forming material in the Nepenthes Mensae unit.

In many instances, map units may consist of diverse, unknown, or uncertain lithologies, which make it difficult to implement a strict rock-stratigraphic approach previously encouraged in Mars geologic mapping (Tanaka and others, 1992b). We find that a more reasonable scheme for mapping complex units on Mars (as well as other planetary surfaces) is to use allostratigraphic units (North American Commission on Stratigraphic Nomenclature, 1983), also known as unconformity-bounded units (UBUs; Salvatore, 1994). This approach discriminates geologic units chiefly by relative age where a significant hiatus can be inferred between overlying and adjacent units. The delineation of geologic units becomes a careful study of age relations along and across mapped contacts. UBUs may commonly consist of multiple lithologies, which are useful when an intimate mixture of diverse lithologies (common to Mars) is impractical to map but where all of these units have geologic and temporal association. For example, though lobate and plains-forming materials of diverse, mixed morphologies in Utopia Planitia (Tinjar Valles a and b units) may include lava and ash flows, lahars, mudflows, and fluvial sediments of complex and variable lithology, they appear to be related to the same period of volcanism and erosion of the west flank of the Elysium rise on the basis of stratigraphic relations and crater counts. Another example is two sets of lava flows in which an older set is faulted by grabens, whereas a younger set buries the grabens. While UBUs have been used in previous Mars geologic maps, the lack of their formal recognition as a unit type, which includes adherence to guidelines for their usage, has resulted in muddled unit definitions and characterizations in some cases. We abandon formal stratigraphic terms such as "formation" and "member" (or "synthem" and "synmember" for allostratigraphic units). We also avoid the term "material" because, most often, the material characteristics are poorly known; instead, we use exclusively the more informal and general term "unit."

These guidelines helped us to determine where map units should be discriminated based on geologic observations and associations and to avoid mapping units that have considerable overlap in both character and age. For example, we do not differentiate between Middle and Late Noachian highland units as mapped previously (Scott and Tanaka, 1986). Although most Noachian surfaces show high variability in crater densities and terrain ruggedness, the variability is generally transitional and

lacks morphologic evidence of embayment relations that suggest distinctive epochs. However, the Early Noachian Libya Montes unit tends to be relatively high standing and densely cratered and appears to be embayed by the less rugged and cratered Noachis Terra unit. Generally, we selected units on the basis of their morphologic characteristics and their association with particular geologic stages, locales, and sources.

UNIT NAMES

We did not use morphology, albedo, terrain type, or any other physical characteristics in map-unit names, because these characteristics can be highly variable and suspect as definitive criteria for unit identification. Instead, units are primarily identified and delineated based on relative age and geologic relations, which makes them incongruent with names based on physical characteristics. We follow a common method employed in terrestrial geologic maps in which units are named after appropriate geographic terms, each of which includes a proper noun and a descriptor-type term (for example, Isidis Planitia unit). The exceptions are crater units, which occur throughout the study area and have consistent and well-characterized morphologies. This approach is comparable to mapping terrestrial alluvium, a unit that is generally not identified with a geographic place name. Because of our limited knowledge of the lithologies of the map units, we do not adopt the terrestrial approach of using a lithologic term (for example, basalt, sandstone) in our unit names.

UNIT GROUPINGS AND SYMBOLS

Previous Mars geologic mappers grouped units using various schemes that incorporated terrain types (lowlands, highlands), volcanic regions, and unit types (channel, aeolian, and surficial materials). On Earth, groups of geologic units generally have local associations, leaving stratigraphers to concern themselves with how isolated sequences might correlate in both space and time. We feel that a similar approach is sensible for most units in the northern plains of Mars, wherein we distinguish six provinces of geologic activity (fig. 1): Amazonis, Elysium, Tharsis, Isidis, Chryse, and Borealis provinces. Remaining units, referred to as widespread materials, have wide spatial occurrence and cannot be delineated by region.

Using the informally named provinces to group units and our unit-naming approach, we propose a symbol scheme as follows: (1) the chronologic period(s) is shown by a large capital letter(s) (A, Amazonian); (2) the province, where applicable, is designated by a small capital letter (B, Borealis province); (3) the unit name, a geographic term, is denoted by a lower-case letter of the proper noun part of the name (v, Vastitas Borealis unit); and (4) sequential and facies subdivisions are shown by number or letter subscripts, respectively. Thus, the geologic symbol ABv_i denotes the Vastitas Borealis interior unit of Amazonian age in the Borealis province.

UNIT COLORS

Most geologic maps follow a color scheme in which units are grouped by lithology or physical characteristics. We use unit colors to stress relative-age information; the natural violet to red spectrum represents oldest to youngest units. Relatively sharp, pure colors are used for units that are specific to a particular epoch and (or) depositional province. Conversely, muted, mixed hues are applied to units of broad temporal and (or) spatial extent. For example, the Late Hesperian units of the Chryse province are represented in shades of vibrant blue while Noachian units of broad areal extent are represented in mixed hues that result in shades of muted brown. As a result of this color scheme, visual inspection provides a general sense of the ages, age range, and areal extent of map units and removes the interpretive bias of color schemes based on inferred origins.

CONTACT TYPES

We attempt to carefully define and delineate map contacts using certain, approximate, gradational, inferred, and inferred approximate contacts. A certain contact denotes the most precise contact between well-characterized material units that contrast in appearance and (or) relative age. Alternatively, an approximate contact is less precisely located due to data quality, subtlety of the contact, and (or) secondary surface modification, where the existence of the contact is generally not in question. A gradational contact is used around composite units consisting of mixtures of older materials and their apparent erosional products, such as older knobby material surrounded by younger plains material; such units grade with adjacent, continuous outcrops of both the older material and younger plains-forming material at the base of the knobs. An inferred contact is used when the uniqueness of two units is uncertain, for example the contact between the Vastitas Borealis interior and marginal units. The units may be of similar origin but modified in different manners, or they may have fairly distinctive origins and (or) ages. An inferred approximate contact is used where an inferred contact cannot be placed precisely.

FEATURE SYMBOLS

The map includes a variety of morphologic feature symbols, following precedents generally established in previous geologic maps of Mars. Mapped linear features are generally >150 km long. In addition, we subdivide our mapping of some features as indicated in the Explanation of Map Symbols. Although consistent mapping of features is desired, it is generally not possible or practical. Factors that complicate the consistent mapping

of features include locally rugged terrain; variation in feature character, length, and relief; feature orientation versus illumination direction; and areas of low data resolution and quality. In addition, the features themselves commonly grade in appearance, and overlaps in feature identification occur (for example, troughs may be similar to channels, whereas scarps may have the same appearance as asymmetric ridges). For ridges and troughs, we delineated subdued varieties, which tended to lack detail and whose bounding slopes were generally modest (see also Structure and Modification History section). Some of the features may have multiple origins and must be interpreted with care. We also chose to show polar residual ice on and around Planum Boreum as a stipple pattern using a mosaic of spring and summertime MOC wide-angle images, because the ice is only meters thick (and has no obvious topographic expression at MOLA resolution), is identified by albedo, and varies in extent from year to year. Polygonal fractures (for example, Adamas and Cydonia Labyrinthi) and thumbprint terrain (for example, east of Davies* crater) are represented by patterns in most areas, because the fractures and troughs and irregular ridges of these features are generally too small to map individually. Collectively, however, the structures cover extensive expanses of the Vastitas Borealis units.

GIS APPROACHES AND TOOLS

Our mapping procedures relied heavily on GIS software and techniques, which provided us with enhanced visualization, mapping tools, and analytical capabilities. We were able to import in common projection the MOLA, MOC, and Viking data and derive MOLA-based thematic maps upon which to map and to readily perform comparative analysis among the datasets. Some datasets had to be processed and (or) reprojected using USGS Integrated Software for Imagers and Spectrometers software. This software can be obtained online at http://isis.astrogeology.usgs.gov/. We stream digitized our original line work with a vertex spacing of 3 km in most cases.

STRATIGRAPHY

Although the geology of all or parts of the northern plains region of Mars was mapped variously at 1:15,000,000 or larger scale using Viking Orbiter images (Scott and Tanaka, 1986; Greeley and Guest, 1987; Tanaka and Scott, 1987), significant improvements in image and topography data resolution, quality, and positioning accuracy and in mapping techniques permit a substantially revised and better-constrained stratigraphy. Some initial results of our mapping were presented in Tanaka and others (2003b); however, this map reflects many modifications and improvements over that preliminary work. We attempt to limit the discussion of morphologic and other physical properties to those thought to be intrinsic to the unit when formed; unit modification features are discussed in the Structure and Modification History section.

Stratigraphic relations among the map units are comprehensively summarized in table 1, which provides relative-age information determined by contact relations observed in mapping datasets. Although we are generally confident with these results, we caution that subtle relations may be missed or incorrectly inferred, especially where the contact is uncertain. In addition, some units are likely to have formed over considerable periods of time and (or) are partly buried. As a result, some units may not be fully and (or) properly characterized. Furthermore, some units that have undergone modest resurfacing following their initial formation may have obscure or even reversed apparent stratigraphic age relations; we largely ignore such modifications where the scale of the mapping precludes presenting such details.

In table 1, crater densities were derived using computed map unit areas and Barlow's crater database, which includes crater size, location, and morphologic characteristics (N.G. Barlow, 1988, and written commun., 2003). Map units were assigned to the eight Martian epochs on the basis of the scheme of Tanaka (1986) for the number of craters >5 and >16 km in diameter per million square kilometers (N(5) and N(16), respectively), as well as on stratigraphic relations and our understanding of the crater retention history for given unit surfaces. As noted in table 1, some units may be relatively thin (tens of meters to a few hundred meters thick) and have anomalously high crater densities due to significant numbers of craters included in the counts that are actually embayed or thinly buried by the unit. In addition, ages reported for populations of subkilometer-sized craters may be generally suspect due to a preponderance of secondary craters in this size range (McEwen and others, 2005).

We discuss the map units in stratigraphic order starting with the oldest units, based on their age of onset (which is commonly only approximately understood). Many of the key relations are shown in the work of Tanaka and others (2003b). Although geologic cross sections are generally helpful in elucidating vertical and lateral relationships between map units, we have not produced sections for this map, because the subsurface geology of most of the map area is poorly known and likely highly variable. An example of a schematic cross section across southern Utopia Planitia that is consistent with our mapping results and inferences is shown in Tanaka and others (2003a, fig. 9).

EARLY NOACHIAN EPOCH

The Early Noachian represents the period of oldest exposed rocks on Mars. Older, pre-Noachian rocks of the primordial crust produced during early planetary differentiation likely underlie and may be constituents of Noachian rocks. The "quasi-circular depressions" that are

tens to hundreds of kilometers in diameter in both highland and lowland regions around Mars may represent a population of buried impact basins occurring within such pre-Noachian rocks (Frey and others, 2002; Frey, 2004; Nimmo and Tanaka, 2005).

Libya Montes unit

The Libya Montes unit (Nl) represents the oldest exposed rocks in the map area, forming the rugged, densely cratered massifs of Libya and Xanthe* Montes and rugged cratered terrain near Nili Fossae and Amenthes Rupes and in Xanthe* and eastern Margaritifer Terra. We map the extent of the unit where carved by Kasei and Ares Valles by assuming that the unit surface dips gently away from nondissected unit surfaces, which is consistent with a geometry of materials raised by impact and (or) tectonic processes. The Libya Montes unit appears embayed by all adjacent materials, including the Noachis Terra unit (Nn) in most places (however, the contact is generally obscured due to resurfacing), and includes highly degraded crater features. The rugged, high-standing character of the Libya Montes unit likely makes it susceptible to erosion, possibly accounting for its similar densities of observed craters relative to those of the Noachis Terra unit (table 1). Also, parts of the unit likely extend into the Middle Noachian. These materials may have formed from uplifted ancient crustal materials where they are in proximity to large, ancient impact basins, including the Isidis and putative Chryse Planitia structures (Schultz and others, 1982); alternatively, Xanthe Montes* may be related to ancient tectonism of the Tharsis rise or other tectonism (Fairén and Dohm, 2004).

Nepenthes Mensae unit

The Nepenthes Mensae unit (HNn) includes (1) material forming knobs and mesas of Nepenthes, Nilosyrtis, and Protonilus Mensae; Phlegra, Erebus, and Tartarus Montes; Tartarus Colles; and Cydonia and Aeolis Mensae (outside the map area) and (2) slope and plains deposits between the knobs and mesas. Unit outcrops are as much as a few hundred kilometers wide and thousands of kilometers long. Individual knobs and mesas range from less than a kilometer to a few tens of kilometers in width and up to a few kilometers in relief. The base of the unit occurs at elevations of –2,000 to –4,000 m and has a relief that locally approaches 3,000 to 4,000 m. The material of the mesas and knobs include Noachian materials equivalent to the Libya Montes and Noachis Terra units (Nl and Nn), whereas the intervening slope- and plains-forming materials were emplaced during the Late Noachian and into the Early Hesperian. The Nepenthes Mensae unit may be mass-wasted talus, slide, and flow materials. Depressions within the unit indicate that collapse occurred due to displacement and (or) removal of subsurface material (Tanaka and others, 2003b). Additionally, Parker and others (1989, 1993) hypothesized that ancient oceans filled the northern plains and eroded the coastlines, producing the dense knobs and intervening deposits.

MIDDLE AND LATE NOACHIAN EPOCHS

Noachis Terra unit

Many Viking-based geologic maps of Mars distinguish various Middle and Late Noachian highland materials, using relative crater density and occurrence of morphologic features such as valleys, fractures, and other features (Scott and Tanaka, 1986; Greeley and Guest, 1987; Tanaka and Scott, 1987). We find, however, that in most heavily cratered highland regions along the lowland margin, the clear and consistent discrimination of Middle versus Late Noachian outcrops is problematic due to a lack of potential embayment features such as slight elevation differences, for example subtle scarps, between areas of relatively high and low crater density. As a result, we map a single unit, the Noachis Terra unit (Nn), to represent broad expanses of heavily cratered material that apparently embays the higher relief Libya Montes unit (Nl). The timing of contacts between the Libya Montes and Noachis Terra units cannot be precisely dated, therefore extensive temporal overlap between the units is possible and likely. Degraded crater material within the unit also is not mapped separately as in previous maps, because the unit is generally interpreted to consist of crater material in addition to local deposits of aeolian deposits, alluvium, volcanic rocks, and other materials that, in most cases, cannot be confidently differentiated. In MOC narrow-angle images, much of the unit displays layering (Malin and Edgett, 2001). The unit occurs in highland terrains in the elevation range of –3,000 to 5,000 m above and surrounding the northern plains; it also occurs within the northern plains at Orcus Patera and Acidalia Mensa, between –2,000 and –5,000 m in elevation.

Lunae Planum unit

Southern Lunae Planum (outside the map area) includes lobate flows and local rille structures that may be volcanic channels (Witbeck and others, 1991). Where cut by Coprates Chasma, a series of thick layers thought to be lava flows form a sequence a few kilometers thick (McEwen and others, 1999). We consider that the Lunae Planum unit (HNTl) in northern Lunae Planum also consists of a considerable thickness of lava flows and, perhaps, other volcanic-related materials, where layering has also been detected in Viking images (Scott, 1991; Tanaka and Chapman, 1992). Such thick sequences of lava flows may point to a Europe-sized, Noachian basin with Valles Marineris as its central part (Dohm and others, 2001a). Thus, where Kasei Valles dissects the Lunae Planum unit, we show that the channel floor exposes a kilometer-

thick sequence of the unit (Tanaka and Chapman, 1992) between about –2,000 and –1,000 m in elevation, part of which may be Late Noachian and older.

Chryse Planitia 1 unit

Chryse Planitia 1 unit ($HNCc_1$) consists of high-elevation (mostly –3,500 to –2,000 m), plains-forming material that embays the Libya Montes and Noachis Terra units (Nl and Nn) and kilometer-scale remnant knobs and mesas of Noachian material along the lowland margins of Chryse and Acidalia Planitiae. Chryse Planitia 1 unit appears to result from mass wasting and local fluvial dissection of northern Xanthe and Margaritifer Terrae during the Late Noachian to Early Hesperian. The unit appears to be similar in age and origin to the Nepenthes Mensae unit (HNn), but consists of significantly less Noachian relict material and features and possibly a greater proportion of fluvial material.

EARLY HESPERIAN EPOCH

Crater and crater floor units

Throughout the map area, impacting bolides formed craters whose rims and ejecta, including rampart margins and secondary craters, presently remain relatively well preserved. Presumably, such craters postdate the Noachian, when erosion rates across the entire planet may have been significantly higher (Craddock and Maxwell, 1993; Craddock and Howard, 2002). These craters, therefore, do not belong to the Noachis Terra unit (Nn) and are mapped as the crater unit (AHc). They range in age from Early Hesperian to Late Amazonian and mostly overlie adjacent units. Because some adjacent units are thinner than crater ejecta rampart margins, as seen in MOC narrow-angle images, some well-preserved craters actually predate adjacent units. As a result, crater-density data for such units should be viewed with caution (see table 1). Also, many degraded craters largely within the Libya Montes (Nl) and Noachis Terra units were infilled by plains-forming material mapped as the crater floor unit (AHcf) that may include aeolian dust and sand, volcanic ash, and fluvial deposits of post-Noachian age. MOC images indicate that many exposures of the crater floor unit are composed of finely layered, friable materials (Malin and Edgett, 2001). The outcrops within Aram Chaos are associated with hematite-rich material as determined by the MGS Thermal Emission Spectrometer (TES) (Christensen and others, 2001).

Deuteronilus Mensae 1 unit

Deuteronilus Mensae 1 unit (HBd_1) forms the low-lying plains within the fretted troughs and broad depressions bounding the large mesas and knobs of Deuteronilus Mensae along the margin of the highland/lowland boundary. This unit embays the Noachis Terra unit (Nn) in the Deuteronilus Mensae region and the Nepenthes Mensae unit (HNn) southeast of Lyot crater; the Vastitas Borealis marginal and interior and Deuteronilus Mensae 2 units (ABv_m, ABv_i, and ABd_2) embay the Deuteronilus Mensae 1 unit. These observations are consistent with the Early Hesperian age assigned to the formation of fretted channels by McGill (2000). The channels and mesas appear to have formed by downslope, subsurface flow of ice-rich material, which removed the supportive substrate and resulted in collapse (Sharp, 1973; Lucchitta, 1984). Spring-fed ground-water discharge during warm-climate periods may have also contributed to fretted channel development.

Utopia Planitia 1 unit

Throughout the southern and western marginal zone of Utopia Planitia and in an area of southwestern Amazonis Planitia, the Nepenthes Mensae unit (HNn) grades into Utopia Planitia 1 unit (HBu_1), which is dominated by (1) plains-forming material that appears rugged at ten- to hundred-meter scales and (2) sporadic knobs generally smaller than those in the Nepenthes Mensae unit. Utopia Planitia 1 unit occurs mostly at elevations of –3,000 to –2,000 m. Small pancake-shaped mesas with interior knobs and thin flows occur locally within the unit in southern Utopia Planitia and may be the result of mud or magmatic volcanism (Tanaka and others, 2003a) that may represent minor activity late in unit formation. Locally, smooth deposits embay cratered and hilly surfaces within the unit. Crater counts (table 1) indicate that Utopia Planitia 1 unit is younger than the Nepenthes Mensae unit. Utopia Planitia 1 unit likely consists of the reworked, distal, coalesced debris shed from highland-boundary degradation associated with formation of the Nepenthes Mensae unit.

Amenthes Planum unit

Amenthes Planum*, a broad, northwest-trending trough on the west side of Amenthes Rupes, is covered by the Amenthes Planum unit (Hla). The unit ranges from about –2,000 to 0 m elevation and embays outcrops of the Noachis Terra and Nepenthes Mensae units (Nn and HNn). The unit generally lacks distinctive primary morphologies except for local channels and scarps seen in THEMIS visible images. The unit may be made up of fluvial sediments and volcanic flows originating from local sources. Its contact with Utopia Planitia 1 unit (HBu_1) is not clearly defined, and the Amenthes Planum unit may extend farther into Isidis Planitia than mapped.

Syrtis Major Planum unit

Lobate flows mapped as the Syrtis Major Planum unit (Hls), some with pronounced medial ridges with crestal fissures, cover Syrtis Major Planum and likely erupted from Nili and Meroe Paterae and local frac-

tures. The flows reach the west margin of Isidis Planitia, where they appear locally cracked and eroded; some have a broad ridge-like form with pits and channels on their crests (Ivanov and Head, 2003). Overall, flows of Syrtis Major Planum have an Early Hesperian crater age (Tanaka, 1986; Hiesinger and Head, 2004), but a lower density of craters on the east flank of the planum (table 1) suggests that those flows are partly Late Hesperian, which indicates an extensive duration of volcanism. Our mapping observations and crater counts indicate that the Syrtis Major Planum unit predates the Isidis Planitia unit (AIi); however, Ivanov and Head (2003) derive the opposite result, suggesting that the Syrtis Major Planum flows were emplaced on top of the Isidis Planitia unit.

Arcadia Planitia unit

In western Arcadia and Amazonis Planitiae, the Arcadia Planitia unit (HAa) consists of plains material with small knobs and lobate margins in many areas. The unit embays the Nepenthes Mensae and Noachis Terra units (HNn and Nn). The Arcadia Planitia unit appears to be composed of a mixture of colluvium from local mass wasting of the Nepenthes Mensae unit, lava flows associated with Elysium rise and (or) local vents, and perhaps fluvial sediments from dissection of Marte and Mangala Valles (Tanaka and Chapman, 1990). Flows of the Elysium rise unit (AHEe) overlap the Arcadia Planitia unit on its western margins.

Chryse Planitia 2 unit

Plains-forming outcrops of Chryse Planitia 2 unit (HCc_2) in Chryse Planitia may result, in part, as colluvium shed from older, adjacent units; however, most of the unit probably consists of deposits derived from scouring of Maja, Ares, Kasei (and associated fossae), Shalbatana, Bahram, Vedra, and Maumee Valles and perhaps from early, unpreserved scouring of Simud and Tiu Valles. The unit also includes rugged, high-standing, channel-floor deposits in northern Kasei Valles likely made up of channel material and perhaps debris shed from backwasting of the Lunae Planum unit (HNTl) and Noachian wall rocks.

LATE HESPERIAN EPOCH

Simud Vallis unit

The Simud Vallis unit (HCs) consists of material forming chaotic terrain within Xanthe and Margaritifer Terrae, including Hydraotes and Aram Chaos, as well as the chaotic and hummocky floors of Simud and Tiu Valles. Chaotic terrains include mosaics of large mesas and knobs within depressions hundreds to a few thousands of meters deep. Chaos depressions disrupt Noachian materials and outcrops of the crater floor unit. Chaotic terrains are generally thought to be the source of water, water or CO_2-charged slurry, or ice that led to the formation of the outflow channels (Sharp, 1973; Baker and Milton, 1974; Carr, 1979; Nummedal and Prior, 1981; Witbeck and others, 1991; Tanaka, 1997, 1999; Hoffman, 2000). Given this interpretation, the unit appears to be mainly Late Hesperian in age, coeval with Chryse Planitia 3 and 4 and Ares Vallis units (HCc_3, HCc_4, and HCa); some parts may also be synchronous with earlier Chryse Planitia units. Amazonian unit development is possible but has not been clearly demonstrated.

Elysium rise unit

Extensive lava flows of the Elysium rise mapped as the Elysium rise unit (AHEe) erupted from Elysium Mons, Hecates and Albor Tholi, and other local sources. The oldest exposed flows appear to predate Utopia Planitia 2 unit (HBu_2) in southern Elysium Planitia and northeast of Hecates Tholus and to underlie Tinjar Valles a and b units (AEt_a and AEt_b) and the Vastitas Borealis marginal unit (ABv_m) in eastern Utopia Planitia. Older, buried volcanic materials of the Elysium rise could predate the Late Hesperian (Tanaka and others, 1992a). Amazonian flows of the Elysium rise unit overlie the Arcadia Planitia unit (HAa) in western Arcadia Planitia and the Vastitas Borealis interior unit (ABv_i) in southern Utopia Planitia.

Utopia Planitia 2 unit

Along the south and west margins of Utopia Planitia and the south margin of Elysium Planitia, the Utopia Planitia 2 unit (HBu_2) consists of plains material formed topographically lower than Utopia Planitia 1 unit (HBu_1). Utopia Planitia 2 unit is marked by depressions and scarps up to tens of kilometers across and with relief of hundreds of meters. Likely, collapse, degradation, and downslope movement of lower exposed parts of Utopia Planitia 1 unit led to emplacement of Utopia Planitia 2 unit as colluvium (Tanaka and others, 2003a,b). In southern Isidis Planitia, Utopia Planitia 1 unit is absent, perhaps because of the high relief of Libya Montes and overprinting by Utopia Planitia 2 unit, which may consist of detritus from Noachian rocks making up Libya Montes (Crumpler and Tanaka, 2003). Where the outcrops of Utopia Planitia 2 unit in southern Elysium Planitia are isolated within younger materials, their origin and source is uncertain.

Ares Vallis unit

The Ares Vallis unit (HCa) forms pitted, discontinuous, irregular, low plateaus above surrounding plains and channel floors. In THEMIS night-time infrared images, the outcrops appear distinctively bright, indicating relatively warm temperature and high thermal inertia. Outcrops of the unit extend from Iani Chaos (south of Ares Vallis, outside of the map area) into Ares Vallis and southern Chryse Planitia. The unit overlies Noachian materials, Chryse Planitia 1 unit ($HNCc_1$), and, in one

place, Chryse Planitia 2 unit (HCc_2). The pitted morphology may be due to thermokarst processes (Lucchitta, 1985; Costard and Kargel, 1995), which acted on material that may have had a relatively resistant surface due to cementation or some other process. Much of the unit, where not dust covered, has an olivine-rich signature in TES spectra indicative of an igneous origin (Rogers and others, 2005).

Chryse Planitia 3 unit

The Chryse Planitia 3 unit (HCc_3) forms a broad plain at the mouths of Kasei and Maja Valles; plains surrounding the lower, distal reach of Ares Vallis; and scattered, relatively smooth deposits in lower parts of Kasei and Ares Valles. The unit embays Chryse Planitia 2 unit (HCc_2) and the Ares Vallis unit (HCa). The larger outcrops most likely consist of sediments from Kasei, Maja, and Ares Valles. The relative age between sediments of Kasei and Maja Valles is uncertain; the higher density of wrinkle ridges below Maja Valles may mean that the unit in that area is older or perhaps thinner or that it underwent higher contractional strain. The small patches within Kasei and Ares Valles may be fluvial sediments and (or) later aeolian deposits (Tanaka and Chapman, 1992).

Chryse Planitia 4 unit

Chryse Planitia 4 unit (HCc_4) forms the lowest plains in Chryse Planitia and includes irregular fractures and low, convex margins as seen in Viking and THEMIS images. The unit occurs within the relatively lowest channel floors that dissect Chryse Planitia 1–3 units ($HNCc_1$, HCc_2, and HCc_3) and the Ares Vallis unit (HCa) and is cut by chaos structures of the Simud Vallis unit (HCs). The contact with Chryse Planitia 3 unit is uncertain east of the Kasei Valles mouth, making the relative ages of the units uncertain in that area. Chryse Planitia 4 unit includes north-trending streamlined forms that show that the deposit originated from the Simud/Tiu Valles channel system; tongues of the unit bury part of lower Ares Valles. The lobate margins, fractures, and possible mud-volcano structures associated with the unit are consistent with an origin as sediment-laden flood or debris-flow deposits (Tanaka, 1997, 1999).

Chryse Planitia 3 and 4 units (HCc_3 and HCc_4) formed near the end of the Hesperian, because they predate the Vastitas Borealis marginal unit (ABv_m) according to embayment relations and crater densities. Tanaka and others (2003b) suggested that the Vastitas Borealis units resulted from water and gas discharges from reservoirs beneath the plains, as well as from local periglacial processes acting on outflow channel sediments and other older plains materials. However, it remains possible that early Chryse Planitia deposits either are buried beneath the Vastitas Borealis units or were later reworked to form the Vastitas Borealis units; this interpretation is consistent with the hypothesis that the Vastitas Borealis units represent ocean sediments derived from material discharged from the Chryse channels (Parker and others, 1989, 1993; Baker and others, 1991; Kreslavsky and Head, 2002).

Amazonis Planitia 1 south unit

The Amazonis Planitia 1 south unit ($AHAa_{1s}$) forms relatively smooth, locally lobate plains in southern Amazonis Planitia. It buries the Arcadia Planitia unit (HAa) and is superposed by younger Amazonis Planitia units and the Medusae Fossae unit (AAm). The unit may represent Late Hesperian to Early Amazonian lava flows and (or) sediment from Mangala Valles (Tanaka and Chapman, 1990) or other local sources.

Alba Patera unit

Lobate shield flows on the north flank of Alba Patera are mapped as Alba Patera unit (HTa). The flows embay the Noachis Terra and Nepenthes Mensae units (Nn and HNn) and have a Late Hesperian crater density. Some of the more pronounced, distal flows include medial channels. One extensive flow underlies Milankovič crater ejecta; the flow's relative age to the Vastitas Borealis marginal unit (ABv_m) is uncertain.

EARLY AMAZONIAN EPOCH

We redefine the Hesperian and Amazonian boundary. Based on Mariner 9 geologic mapping, Scott and Carr (1978) assigned the beginning of the Amazonian to the base of their "cratered plains material" mapped across much of the northern plains and less cratered parts of the Tharsis rise and southern highlands. Using Viking-based mapping (Scott and Tanaka, 1986; Greeley and Guest, 1987; and Tanaka and Scott, 1987), Tanaka (1986) assigned the beginning of the Amazonian to emplacement of smooth plains material lying in southern Acidalia Planitia and defined their Vastitas Borealis Formation as Late Hesperian. We interpret the plains material in southern Acidalia Planitia as an extension of the plains material in Vastitas Borealis, which we map as Vastitas Borealis marginal and interior units (ABv_m and ABv_i). We use these units to define the base of the Amazonian, and their crater densities are still fairly consistent with the N(5) = 67 definition of Tanaka (1986) for the beginning of the Amazonian. Because of their extent and apparent uniform age, the Vastitas Borealis units seem to express a broad, significant, yet brief episode of geologic activity for the planet and are better suited for defining such a significant stratigraphic boundary.

Vastitas Borealis interior unit

The Vastitas Borealis interior unit (ABv_i) consists of relatively bumpy, plains-forming material in the MOLA DEM and in 100-m/pixel-resolution THEMIS images.

The unit covers most of the northern plains including Vastitas Borealis and Utopia, Acidalia, and northern Arcadia Planitiae. Younger materials bury the unit in eastern and central Utopia Planitia, in Amazonis and southern Arcadia Planitiae, and in the northern polar region. The outer, higher parts of the interior unit include sets of parallel, arcuate ridges composed of pitted cones, commonly referred to as "thumbprint terrain," as well as random clusters of hills mostly <1 km across (Frey and Jarosewich, 1982; Grizzaffi and Schultz, 1989; Scott and others, 1995). The cones were first interpreted as possible pseudocraters formed by explosions associated with lava emplacement over wet ground (Frey and Jarosewich, 1982; Carr, 1986), cinder cones (Scott and others, 1995), pingoes, ice-cored ridges (Lucchitta, 1981; Rossbacher and Judson, 1981), moraines (Lucchitta, 1981; Scott and Underwood, 1991; Kargel and Strom, 1992; Lockwood and others, 1992), or mounds formed by the disintegration of stagnant ice covers (Grizzaffi and Schultz, 1989). More recently, they were interpreted as mud volcanoes (Tanaka, 1997; Tanaka and others, 2003b). Within a few hundred kilometers of the edge of the interior unit, the pitted cones become more widely spaced and tend to occur in small groups or individually until they disappear entirely. Here, polygonal trough systems (representative ones are mapped as fresh troughs) begin to appear, characterizing the surface of interior, apparently unmantled lower elevation regions of the interior facies such as Adamas Labyrinthus in central Utopia Planitia and in the plains surrounding Planum Boreum as seen in the 256-pixel/degree MOLA DEM. Also, the well-developed polygonal troughs of Cydonia Labyrinthus occur within a shallow depression. The polygonal troughs may form by desiccation and (or) compaction of wet sediment (Lucchitta and others, 1986; McGill and Hills, 1992).

Vastitas Borealis marginal unit

The Vastitas Borealis marginal unit (ABv_m) consists of plains-forming material that appears smooth in the MOLA DEM and in 100-m/pixel-resolution THEMIS images. The unit forms patches marginal to most of the Vastitas Borealis interior unit (ABv_i) in Utopia Planitia, along Arabia Terra, in southern Acidalia Planitia, north of Alba Patera, and in western Arcadia Planitia. Where the marginal unit onlaps plains units such as Utopia Planitia 2 unit (HBu_2) and Chryse Planitia 2–4 units (HCc_2, HCc_3, and HCc_4), the edge of the unit has a broad, lobate form with individual lobes commonly several kilometers across that wrap around small knobs in many cases. Narrow ridges outline some of the margins of the lobes. At lower latitudes (<25° N.), the marginal unit appears generally brighter and, thus, warmer than adjacent materials in THEMIS daytime infrared images, which may indicate a bulk surficial content of relatively fine-grained material compared to underlying or adjacent materials. Materials of the Amazonis and Elysium provinces bury parts of the unit. The marginal unit includes local systems of narrow sinuous troughs (larger ones are mapped as subdued troughs) that are a few kilometers wide and tens of kilometers long and have low medial ridges; in some cases, the troughs form intricate networks such as Pyramus Fossae in northwestern Utopia Planitia and similar features in western Arcadia Planitia (Tanaka and others, 2003b). These features have no clear terrestrial analogs and have been compared to glacial moraines and kame complexes (Lucchitta, 1982), glacial tunnel-valley and esker features (Kargel and others, 1995), or soft-sediment deformation structures (Tanaka, 1997; Tanaka and others, 2003b). Stratigraphic and topographic relations indicate the features likely formed soon after unit emplacement and may have deformed the substrate as well.

The Vastitas Borealis marginal and interior units generally have a readily mappable but poorly understood contact and post-emplacement modification histories. We mapped it as an inferred contact because the two units possibly represent a once continuous deposit that either (1) was reworked into distinctive material units or (2) has retained its essential stratigraphic character and is a single unit with variable and distinctive secondary modification. The collective outer margin of the Vastitas Borealis units displays a fairly constant elevation that may indicate the former presence of a standing body of water (Parker and others, 1989, 1993; Head and others, 1999; Clifford and Parker, 2001; Carr and Head, 2003) or a common groundwater table (Tanaka and others, 2003b).

Isidis Planitia unit

The Isidis Planitia unit (AIi) covers most of Isidis Planitia, shares similar morphologic features with the Vastitas Borealis units (ABv_m and ABv_i) in the Borealis province, and is separated from the Borealis province by a narrow (<150 km) strip of the Utopia Planitia 2 unit (HBu_2) that covers a low saddle between Utopia and Isidis basins (Tanaka and others, 2003b). We do not distinguish marginal and interior units, because the features distinguishing them in the Borealis province appear intimately mixed. Trough features occur on the northwestern and southwestern marginal areas of the unit, whereas the remainder of the unit includes distinct sets of ridges of pitted cones of greater relief and steeper flanks than those in the Vastitas Borealis interior unit (Tanaka and others, 2003b). Along the Isidis Planitia unit contact with the Syrtis Major Planum unit (HIs), the Isidis Planitia unit locally includes pitted cones and ridges occurring along fractures within the Syrtis Major Planum unit. The crater density of the unit indicates an Early Amazonian age, and it may be coeval with the Vastitas Borealis units. The Isidis Planitia unit and its features generally share the same interpretations as the Vastitas Borealis units with the addition that Grizzaffi and Schultz (1989) inter-

preted its pitted cones as moraine remnants of an ice-rich debris layer.

Medusae Fossae unit

The Medusae Fossae unit (AAm) covers parts of southern Elysium and Amazonis Planitiae and the Tharsis rise. This material is characterized by a sequence of layers that appear to be etched by the wind to form streamlined yardang mounds; the consistent, sometimes cross-cutting trends of the mounds indicate that they may result from preferential erosion along cracks (Tanaka and Golombek, 1989). THEMIS daytime infrared images show isolated patches of the unit within Elysium and southern Amazonis Planitiae. Dating the unit by crater counts is tenuous because of the high degree of erosion; stratigraphic relations with Tharsis flow materials indicate that the Medusae Fossae unit spans much of the Amazonian (Scott and Tanaka, 1982, 1986; Greeley and Guest, 1987). In the map area, the unit buries Amazonis Planitia 1 south unit ($AHAa_{1S}$) and some Noachian and Hesperian materials, and it appears to both predate and postdate adjacent Middle and Late Amazonian units. The unit has a variety of interpretations, including explosive volcanism (Scott and Tanaka, 1982; Tanaka, 2000; Hynek and others, 2003), a hypothesis consistent with the geologic setting of the unit. Alternatively, the unit may be a highly erodible aeolian deposit (Scott and Tanaka, 1986; Greeley and Guest, 1987) or other fine-grained deposits.

Tinjar Valles a and b units

Superposed on the Vastitas Borealis units in Utopia Planitia are lobate deposits of Tinjar Valles a and b units (AEt_a and AEt_b). Tinjar Valles a unit consists of rugged material forming lobes dissected by Hrad, Apsus, Tinjar, and Granicus Valles, whereas Tinjar Valles b unit includes relatively smooth material within and lining parts of the channels. The Tinjar Valles units collectively form a broad tongue of material extending >1,500 km from the northwest flank of the Elysium rise into the central floor of Utopia basin. These Early Amazonian deposits are interpreted to have been emplaced as lahars and (or) other volcanic or debris flows that resulted from the intermingling of magmatism and subsurface volatile reservoirs along the deep troughs of Elysium Fossae (Christiansen, 1989; Tanaka and others, 1992a; Russell and Head 2003).

Scandia region unit

Deep within Borealis basin and on top of the Vastitas Borealis interior unit, the Scandia region unit (ABs) forms (1) much of the base of Planum Boreum and (2) a complex of mesas, knobs, and circular and irregular patches of material in Vastitas Borealis north of Alba Patera. In Planum Boreum, the unit occurs mostly west of Chasma Boreale and ranges from hundreds of meters to more than 1,000 m in thickness. In MOC images, these outcrops display dark, crossbedded layers that eroded into debris fans and meter-size boulders and that apparently contributed to the formation of dunes; underlying the crossbedded layers are brighter, platy layers that extend from scarp bases (Malin and Edgett, 2001, 2005; Byrne and Murray, 2002; Fishbaugh and Head, 2005). The unit includes the plateau on the floor of Chasma Boreale that is a few hundred meters thick and displays about 10 layers in THEMIS images; these layers may underlie the crossbedded and platy layers making up upper exposures of the unit in Planum Boreum. The Planum Boreum exposures are superposed by a few craters several kilometers across that are shallowly buried and (or) exhumed from beneath Planum Boreum 1 and 2 units (ABb_1 and ABb_2). This part of the unit may be a sand sea deposit (Byrne and Murray, 2002; Tanaka and others, 2003b; Fishbaugh and Head, 2005), perhaps derived from erosion of the Vastitas Borealis units (ABv_m and ABv_i; Wyatt and others, 2004) and (or) the Vastitas Borealis plains part of the Scandia region unit. The outcrops in Vastitas Borealis are tens of meters to a couple hundred meters thick and form a degraded complex of mesas, knobs (Scandia Colles), and depressions that overlie the Vastitas Borealis and Alba Patera units. Pancake-shaped mesas tens of kilometers across (Scandia Tholi) are partly surrounded by shallow moats. Two large complexes contain the irregular depressions of Scandia Cavi; these outcrops also include irregular ridges and patches of relatively smooth, gently sloping flanks. Scandia Tholi and Scandia Cavi have been interpreted to be formed by eruption of volatile-rich material (Tanaka and others, 2003b); alternatively, some of the larger outcrops have been suggested to be degraded, ice-cored glacial moraines (Fishbaugh and Head, 2001). Locally, terraces that likely represent layering can be observed in the plains outcrops in MOC and THEMIS images; however, much of the unit surface is buried by the thin mid-latitude mantle covering much of the northern plains (Mustard and others, 2001). Steep scarps commonly appear to be mass wasted. We also include in the unit, south of the mouth of Chasma Boreale, irregular mesas and cratered knobs hundreds of meters high that we interpret to be degraded pedestal craters, because their heights coincide with the apparent pre-erosional thickness of the unit. Escorial crater formed on a pedestal as much as 700 m thick in this area (Tanaka and others, 2003b). Alternatively, the cratered knobs also have been interpreted to be volcanoes (Garvin and others, 2000).

Cerberus Fossae 1 unit

The Cerberus Fossae 1 unit (AEc_1) forms a highly fractured, rugged deposit along the south margin of Elysium Planitia. It appears to result from intense deformation of the north margin of the Medusae Fossae unit (AAm; Lanagan, 2004) and predates Middle to Late Amazonian Cerberus Fossae 2 and 3 units (AEc_2 and AEc_3).

Amazonis Planitia 1 north unit

Extending across northern Amazonis Planitia, rugged flows form Amazonis Planitia 1 north unit (AAa_{1n}). The flows emanate from beneath Olympus Mons aureole material (the Lycus Sulci unit, ATl) and bury the Vastitas Borealis marginal and interior, Arcadia Planitia, and Nepenthes Mensae units (ABv_m, ABv_i, HAa, and HNn). The rugged character of the flows is unlike that of typical lava flows; rather, they may be pyroclastic flow deposits, lahar deposits, and (or) surficially modified lava flows. Fuller and Head (2003) proposed that the lavas represent an initial stage of high effusion for the incipient development of Olympus Mons. The crater density suggests an Early to Middle Amazonian age.

MIDDLE AMAZONIAN EPOCH

Lycus Sulci unit

The Lycus Sulci unit (ATl) forms the rugged, corrugated lobes of the Olympus Mons aureole deposits, Lycus Sulci. The unit overlies Amazonis Planitia 1 north unit (AAa_{1n}) and is overlain by part of the Medusae Fossae unit (AAm) and the Amazonis Planitia 2 north and south units (AAa_{2n} and AAa_{2s}). These stratigraphic relations suggest that the unit is Middle Amazonian, which is somewhat younger than previously thought (Morris and Tanaka, 1994). A variety of ideas for the formation of this unit have been proposed; rapid landslides (Lopes and others, 1980; McGovern and others, 2004) or slower gravity spreading of a larger, perhaps ice-lubricated, proto-Olympus Mons edifice (Francis and Wadge, 1983; Tanaka, 1985) are mechanisms incorporating the formation of the Olympus Mons basal scarp.

Deuteronilus Mensae 2 unit

Debris aprons forming Deuteronilus Mensae 2 unit (ABd_2) occur in the Deuteronilus Mensae region; similar aprons occur east of Hellas basin in the southern hemisphere (Greeley and Guest, 1987). The aprons are sparsely cratered and overlap fretted channel floors and the plains of Deuteronilus Mensae 1 and Vastitas Borealis marginal units (HBd_1 and ABv_m). Some outcrops include large inlier mesas of Noachian rocks, which are not included in the age assignment for the unit. The aprons likely result from mass wasting of the walls of the Noachis Terra unit (Nn), which suggests that the Noachis Terra unit is volatile rich in this area (Lucchitta, 1984). The young unit age may indicate that the mass-wasting process remains relatively active (Squyres, 1978, 1979a); initial development of the unit, however, is uncertain and may extend as far back in time as the Late Hesperian.

Amazonis Planitia 2 south unit

The Amazonis Planitia 2 south unit (AAa_{2s}) consists of lobate flows that emanate from vents along the margin of southeastern Amazonis Planitia and extend hundreds of kilometers west and north into the plain. The unit generally appears to embay the Lycus Sulci and Medusae Fossae units (ATl and AAm) as seen in THEMIS images. The northern contact of the unit grades into Amazonis Planitia 2 north unit (AAa_{2n}).

Amazonis Planitia 2 north unit

The Amazonis Planitia 2 north unit (AAa_{2n}) consists of lava flows that form an extremely flat and smooth (in the MOLA DEM; Kreslavsky and Head, 2000) surface in central Amazonis Planitia and that exhibit lava-flow surface textures in MOC images and high radar backscatter (Fuller and Head, 2002). Broad, arcuate, low-relief channels migrate across the unit as seen in MOLA and THEMIS infrared images and may indicate late-stage water floods (Fuller and Head, 2003) or lava channels. The unit embays the Amazonis Planitia 1 north and the Lycus Sulci units (AAa_{1n} and ATl) and large impact craters that the unit surrounds. The source of the unit is uncertain and may include distal extensions of Amazonis Planitia 2 south, Cerberus Fossae 2, and (or) Cerberus Fossae 3 units (AAa_{2s}, AEc_2, and AEc_3).

Cerberus Fossae 2 unit

Cerberus Fossae 2 unit (AEc_2) forms lobate and channelized flows issuing from widely scattered parts of the Cerberus Fossae fracture system and covering parts of eastern Elysium Planitia and terraces along Marte Vallis. The unit is associated with the Grjotá and Rahway Valles* channel systems (Plescia, 2003). Topographically subdued, conical vents occur in the unit along fracture traces in southeastern Elysium Planitia. This unit likely consists of lava flows and fluvial sediments associated with episodes of volcanism and water discharge. The unit embays the Cerberus Fossae 1 unit (AEc_1), Elysium rise unit (AHEe), and other older units. The unit generally appears to be lightly cratered, which indicates a Middle to Late Amazonian age, but its crater count includes many larger craters that appear dissected by the associated channels and, thus, are superposed on underlying material. Much of the unit was dissected and buried by fluvial discharges and lava flows associated with Cerberus Fossae 3 unit (AEc_3; Lanagan, 2004).

LATE AMAZONIAN EPOCH

Cerberus Fossae 3 unit

A large field of lava flows making up Cerberus Fossae 3 unit (AEc_3) extends from sites along southern Cerberus Fossae and associated low shields into Elysium Planitia and Marte Vallis. The flows have a platy, ridged texture resembling the historic Laki flood basalt in Iceland (Keszthelyi and others, 2000). The unit overlies and embays most adjacent units including Cerberus Fossae

1 and 2, Utopia Planitia 1 and 2, and Arcadia Planitia units (AEc_1, AEc_2, HBu_1, HBu_2, and HAa; compare regional mapping with that of Lanagan, 2004). It generally embays the Medusae Fossae unit (AAm), except for a small patch at lat ~4° N., long 152° E. Densities of sub-kilometer-diameter craters indicate that the unit may be a few to 30 Ma (Hartmann and Neukum, 2001). Where the flows originate from Cerberus Fossae, associated channel dissection indicates that water discharge occurred in association with lava eruptions (Burr and others, 2002a,b; Wilson and Head, 2002; Plescia, 2003).

Astapus Colles unit

Along the west margin of Utopia Planitia at lat 38° to 48° N., the Astapus Colles unit (ABa) forms a thin deposit (tens of meters thick) covering the Vastitas Borealis and Utopia Planitia units (ABv_m, ABv_i, HBu_1, and HBu_2). The unit forms a mantle that appears to have retreated around crater rims and ejecta deposits; this retreat has been interpreted as due to thermokarst forming preferentially along superposed crater ejecta margins (Costard and Kargel, 1995). Nearly all craters in MOC narrow-angle and THEMIS images underlie the unit, which suggests a Late Amazonian age. Crater burial relations indicate a unit thickness of 30 to 40 m (McBride and others, 2005). In THEMIS visible and MOC narrow-angle images, the unit appears to have a relatively low albedo and is cracked by polygonal fractures along which nested pits are common; these features appear to be consistent with periglacial and thermokarst origins (Costard and Kargel, 1995). This unit occurs within the latitude band where a youthful, meters-thick, presumably ice-rich, debris mantle seen in MOC narrow-angle images appears to be eroding (Mustard and others, 2001). However, polygonal cracks tend to occur north of lat 55° N. where the MO Neutron Spectrometer detected ice, indicating that the unit formed during a different climate episode that predated the debris mantle (Mangold and others, 2004).

Planum Boreum 1 and 2 units

Planum Boreum 1 and 2 units (ABb_1 and ABb_2) form the upper part of Planum Boreum, some nearby low plateaus, and local crater fill. These units consist of stacks of layers that vary in albedo and (or) thickness, which ranges from about a meter to tens of meters (as seen in MOC narrow-angle images). The units overlie the Scandia region and Vastitas Borealis interior units (ABs and ABv_i). Most of the layers appear to be nearly flat lying, but locally some are folded or tilted and display angular unconformities (Malin and Edgett, 2001). Surfaces of the plateau-capping Planum Boreum 2 unit are mantled by residual, water-rich polar ice. Planum Boreum displays arcuate, swirling trough systems. The troughs display layers of Planum Boreum 1 unit on equator-facing slopes, whereas pole-facing slopes appear to be covered by Planum Boreum 2 unit. Locally, sequences of layers in Planum Boreum 1 unit are truncated along unconformities, indicating uneven deposition and (or) local erosion during accumulation of the unit. Planum Boreum also displays a major re-entrant, Chasma Boreale, containing several deep pits that expose the Scandia region unit below the Planum Boreum units. Two craters approximately 330 and 415 m across (MOC images r0100641 and m2000372, respectively) superpose Planum Boreum 1 unit, and two craters approximately 42 and 90 m across (MOC m2901628) occur on Planum Boreum 2 unit. The paucity of craters on the more widely exposed Planum Boreum 2 unit indicates a surface age of <100 ka (Herkenhoff and Plaut, 2000; Koutnik and others, 2002) and perhaps <20 ka since the previous polar insolation maximum (Laskar and others, 2002). Many studies of the layers, troughs, and chasma suggest a range of contrasting origins and timing relations for their development, involving the planet's obliquity and eccentricity variations; atmospheric volatile and dust transport mechanisms; surface ice; topography; wind activity; ice sublimation, deformation, and melting; and melt-water discharge (Murray and others, 1972; Cutts, 1973; Howard, 1978; Squyres, 1979b; Blasius and others, 1982; Howard and others, 1982; Dial and Dohm, 1994; Benito and others, 1997; Fisher, 2000; Kolb and Tanaka, 2001; Malin and Edgett, 2001; Fishbaugh and Head, 2001, 2002). The Planum Boreum deposits may have formed primarily during the low obliquity and low polar insolation period of the past 5 m.y. (Laskar and others, 2002).

Olympia Undae unit

Surrounding Planum Boreum, dune fields and moderate to low albedo mantles form the Olympia Undae unit (ABo). The 1/256°/pixel- and 1/512°/pixel-resolution MOLA DEMs resolve many of the dunes individually, and dune fields display a distinctive, alternating bright and dark artificial illumination pattern in the shaded-relief images. This pattern is a result of the varying orientation of dune faces to the artificial illumination direction. High-resolution Viking and MOC images of the dunes show barchan and transverse forms (Breed and others, 1979; Tsoar and others, 1979; Malin and Edgett, 2001). The dune seas may be at least several meters thick on average (Lancaster and Greeley, 1990). The unit overlies Planum Boreum 1 and 2, Scandia region, and Vastitas Borealis interior units (ABb_1, ABb_2, ABs, and ABv_i) and locally underlies Planum Boreum 2 unit (ABb_2). Most outcrops of the unit form broad, continuous deposits, but some areas south and west of Olympia Undae include small groups of dunes. The dunes have a low albedo and strong Type 2 TES spectral type (Bandfield and others, 2000) and appear to originate from erosion of Planum Boreum 1 unit (Byrne and Murray, 2002; Wyatt and others, 2004).

No evidence for dune migration over the past 20 years (by comparison of >40 m/pixel Viking Orbiter and <1.5 m/pixel MOC images) has been discovered yet (Malin and Edgett, 2001). In addition, we include mantle material associated with the dunes in the unit. In the MOLA DEM, the mantle material produces a subdued topography over the surface of the Vastitas Borealis interior unit. Within MOC images, the mantle material is locally rippled and appears to embay the dune forms. By nature, this unit is transient and, therefore, young as defined by its present form. However, as a dynamic unit it may have been in existence since the Vastitas Borealis interior and Scandia region units began eroding as early as the Early Amazonian.

Surficial material and properties

Remotely sensed properties of the Martian surface, such as albedo, thermal inertia, topographic roughness, neutron abundance, gamma-ray emissions, and thermal emissivity, relate to intrinsic properties, compositions, and modification signatures of materials of the upper few microns to meters of the surface. In many cases, surface properties reflect recent geologic and climatic activity (Mustard and others, 2001; Head and others, 2003). Mapping and interpreting such properties is generally beyond the scope of this map. One exception is that we have used relative albedo data from MOC wide-angle, defrosted images to document the recent extent of the transient north polar residual ice, which may be meters to tens of meters thick (Malin and Edgett, 2001). The distribution of this material, covering much of Planum Boreum 2 unit (ABb_2) and high-latitude craters and outcrops of the Scandia region unit (ABs), is shown on the map as a white stipple pattern called polar ice (see Explanation of Map Symbols).

STRUCTURE AND MODIFICATION HISTORY

Tectonism, periglacial reworking, collapse, erosion, and other geologic processes that postdate unit emplacement modified materials in the northern plains of Mars. Evidence of geologic processes are mappable and provide a basis for determining age relations among geologic materials and features.

PRE-NOACHIAN

The pre-Noachian period predates the oldest exposed rock record, which begins in the map area with the Libya Montes unit (Nl; Frey, 2004; Nimmo and Tanaka, 2005). One of the earliest structures in the map area is the northern plains basin. Postulated origins for the lowlands include tectonism (Wise and others, 1979; Fairén and Dohm, 2004), a mega-impact (Wilhelms and Squyres, 1984), or a series of large impacts (Frey and Schultz, 1988). In particular, Utopia basin has a circular outline, gravity signature, and associated structure that supports an impact origin (McGill, 1989; Smith and others, 1999) but seems to lack related rock exposures. Free-air gravity anomaly patterns suggest a possible buried impact basin in northwestern Amazonis Planitia (Fuller and Head, 2002). Smaller, quasi-circular depressions tens to hundreds of kilometers in diameter are scattered throughout the lowlands and may be the surface expression of large, buried impacts whose density exceeds that of exposed crater structures (Frey and others, 2002). Thus, many of these structures are likely deeply buried and tectonically relaxed and may date back to the pre-Noachian. Establishment of the northern lowlands likely affected the orientation of the planet's spin axis and greatly influenced subsequent tectonic, volcanic, and volatile-related resurfacing activity.

EARLY NOACHIAN EPOCH

Early Noachian geologic activity affected the Libya Montes unit (Nl). Isidis basin is partly ringed by massifs and heavily cratered terrain of the Libya Montes unit. A large, positive gravity anomaly is centered over the basin, substantiating the impact hypothesis for Isidis basin (Zuber and others, 2000). Xanthe Montes* form a chain of massifs that outline the roughly circular Chryse Planitia and may define a large impact basin (Schultz and others, 1982). However, this interpretation remains speculative as supporting structural evidence is limited and the plain lacks a pronounced gravity anomaly. Alternatively, Xanthe Montes* and the broad ridge they occur on may be due to early Tharsis deformation or, perhaps, some other tectonic origin (Baker and others, 2002; Fairén and Dohm, 2004). MOLA data also demonstrate many subtle basin features tens to hundreds of kilometers across throughout much of the map area (Frey and others, 2002). These earliest features provide topographic and structural controls affecting subsequent geologic activity.

MIDDLE AND LATE NOACHIAN EPOCHS

Noachian and perhaps Hesperian structures that dissect parts of the Libya Montes, Noachis Terra, and Nepenthes Mensae units (Nl, Nn, and HNn) include the arcuate grabens of Nili and Amenthes Fossae, which are concentric with the Isidis basin rim and may relate to tectonic relaxation of the Isidis basin structure (Schultz and others, 1982) or to other structurally controlled processes. Arcuate grabens and normal faults of Acheron Fossae trend along the strike of the broad ridge that they cut. West- to west-northwest-trending grabens cut the Nepenthes Mensae outcrops that comprise Phlegra Montes, Tartarus Montes, and Tartarus Colles east of the Elysium rise. Scarps that deform the Noachis Terra unit throughout the map area may be contractional fold and thrust features that may have developed contemporaneously

with formation of the Noachis Terra unit as a result of global contraction due to planetary cooling (Tanaka and others, 1991; Watters, 1993) and (or) lithospheric bending caused by loading of the northern lowlands (Watters, 2003). Rugged terrain, degradation of structural landforms, and deformation along pre-existing crater-related structures probably have largely obscured much of the contractional deformation within Noachian rocks.

Scattered, sinuous valley systems cut most expanses of Noachian rocks including Tempe, Xanthe, Margaritifer, and Arabia Terrae; Libya Montes; and Terra Cimmeria (Carr and Clow, 1981; Scott and Tanaka, 1986; Greeley and Guest, 1987; Tanaka and Scott, 1987; Craddock and Maxwell, 1993; Scott and others, 1995; Hynek and Phillips, 2001; Craddock and Howard, 2002). Some of these valleys have few tributaries, which may indicate immature drainages established by small outbursts of standing water or by sapping (Carr and Malin, 2000; Irwin and others, 2002) rather than by extensive precipitation-driven overland flow. Relatively subtle drainages can be mapped in high-resolution topographic and image data, resulting in a high density of valley features that may indicate precipitation-fed runoff (Hynek and Phillips, 2003), though constraining the age of these features is difficult in most cases. Overall, it appears that few, if any, of the valleys and their sediments either incise or bury Hesperian units that they encounter along the highland-lowland boundary, though definitive observations remain incomplete. Chryse Planitia 1 unit ($HNCc_1$) may partly represent sediments from this dissection.

Accompanying the formation of the Nepenthes Mensae unit (HNn), arcuate and linear troughs and irregular and circular depressions developed in the adjacent, plateau-forming Noachis Terra unit (Nn), producing a knobby, hummocky terrain. This landscape appears to be formed by fracturing, graben formation, and structurally controlled collapse and mass wasting. The depressions indicate removal of subsurface material, particularly along impact and other structures (Tanaka, 2004; Rodriguez and others, 2005), which suggests that the material was volatile rich. This degradation apparently continued into the Early Hesperian and led to deposition of the Utopia Planitia 1 unit (HBu_1; Tanaka and others, 2003a,b). The Nepenthes Mensae unit resulted from mass wasting of most exposures of the Noachis Terra and Libya Montes units along the highland-lowland boundary, except along the margins of Chryse Planitia. East of the Elysium rise, the Nepenthes Mensae degradation affected low-lying (below –2,000 m elevation) cratered terrain throughout a region that is a few thousand kilometers across. Some of the degradation in southern Amazonis Planitia has been attributed to catastrophic flooding (Dohm and others, 2001a), but the evidence remains obscure. Some planetary scientists have proposed that the northern plains could have been submerged beneath an ocean during the Noachian and into the Hesperian, perhaps due to ground-water flow or precipitation-fed runoff (Clifford and Parker, 2001; Fairén and others, 2003). Though we do not observe any definitive geomorphic evidence for early oceans, the intensity and longevity of resurfacing processes that occurred after ocean formation preclude ruling out their potential existence.

EARLY HESPERIAN EPOCH

Contractional wrinkle ridge and scarp deformation continued to deform nearly all Noachian units and most Early Hesperian units, including the Lunae Planum, Chryse Planitia 1, Utopia Planitia 1, Arcadia Planitia, and Nepenthes Mensae units (HNTl, $HNCc_1$, HBu_1, HAa, and HNn). Ridges within the northern plains may have been developing during this time, perhaps deforming materials underlying the Vastitas Borealis units (ABv_m and ABv_i; Head and others, 2002). Many of the ridges in the Early Hesperian units follow multiple trends, have symmetric cross-sectional forms, seem to be enhanced within the units themselves, and barely extend into nearby outcrops of the Noachis Terra unit (Nn). This might indicate that the strength characteristics in the younger units lead to enhanced strain on fewer structures, whereas strain in older units may be distributed along smaller but more numerous structures. Noachian units may be weak due to impact-related fracturing, grinding, and comminution of ancient target material (MacKinnon and Tanaka, 1989).

Linear, north- to northeast-trending complex grabens and normal faults dissect the Noachis Terra unit of Mareotis and Tempe Fossae, which ranges from Noachian to middle Hesperian (Scott and Dohm, 1990; Moore, 2001) and may relate to rifting along the Tharsis Montes axial trend.

Fretted channels and troughs in the Deuteronilus Mensae region of northern Arabia Terra developed by subsurface flow and withdrawal of presumably ice-rich material (Sharp, 1973; Squyres, 1978; Lucchitta, 1984; McGill, 2000), although other hydrologic phenomena such as spring-fed activity related to climate change in a volatile-rich region may have also contributed to their formation (Baker and others, 1991; Barlow and others, 2001). Locally, some pitted hills within the fretted troughs may be volcanoes resulting from magma/ground-ice interactions (Carruthers and McGill, 1998), rootless cones related to diapirism, mud volcanism related to compaction of volatile-rich sediments (Tanaka and others 2003b), or some other extrusive mechanism.

Within the Vastitas Borealis, Utopia Planitia, and older Chryse Planitia units (ABv_m, ABv_i, HBu_1, HBu_2, $HNCc_1$, and HCc_2), adding the number of degraded craters having flat floors and low or absent rims (fig. 2) to the number of fresh-appearing craters yields crater densities consistent with an Early Hesperian buried surface (Head

and others, 2002). Alternatively, the degraded crater record may be incomplete or the substrate may be complex, and a mixture of Noachian to Late Hesperian surfaces and materials underlie the Vastitas Borealis units.

LATE HESPERIAN EPOCH

Narrow, en echelon grabens of Tantalus Fossae extend hundreds of kilometers and cut the Alba Patera unit (HTa) of northeastern Alba Patera. The Scandia region unit (ABs) buries some of these grabens. Some of the parallel-trending grabens of Tempe and Mareotis Fossae farther east may also have formed at this time. The deformation may involve rifting along the Tharsis Montes axial trend, perhaps stimulated partly by Alba Patera and Tempe Terra volcanism (Scott and Tanaka, 1986; Scott and Dohm, 1990; Tanaka, 1990).

Contractional, symmetric wrinkle-ridge and scarp deformation continued to deform earlier units marked by ridges and scarps, as well as Late Hesperian materials including the Arcadia Planitia, Elysium rise, Chryse Planitia 2 and 3, and Utopia Planitia 2 units (HAa, AHEe, HCc_2, HCc_3, and HBu_2). Ridges in Utopia Planitia 2 unit follow multiple trends and seem to be enhanced within the unit and, perhaps, in adjacent Early Hesperian units, but they barely extend into nearby outcrops of the Noachis Terra unit (Nn). Also, some wrinkle ridges concentric to Alba Patera deform the southern part of the Scandia region unit (ABs) and the outermost flows of the Alba Patera unit (HTa). Such deformation is absent within the inner part of the Alba Patera shield and along the Tantalus Fossae fracture swarm and either may be buried or did not occur. Some of this deformation may be Amazonian.

Collapse of lower parts of Utopia Planitia 1 unit (HBu_1) in southern Utopia Planitia apparently led to formation of the irregular depressions of Amenthes Cavi* and deposition of Utopia Planitia 2 unit (HBu_2). Some of the depressions appear nested and have raised or fractured rims and associated knobs, fractured hills (some with moats), and pitted topography in THEMIS visible images. The fractured hills may be sites of heaving. Both Utopia Planitia units likely were volatile rich. Intensive mass wasting of Noachian, perhaps volatile-rich rocks of Deuteronilus Mensae resulted in knobby plains material of Deuteronilus Mensae 1 unit (HBd_1; Mangold and others, 2002). Some of the older unit surfaces are cut by networks of polygonal fractures spaced hundreds of meters apart, which indicates periglacial ice wedging (Lucchitta, 1985).

Major incision of the circum-Chryse outflow channel system and chaos development occurred at this time, possibly related to a significant pulse of Tharsis magmatism (Dohm and others, 2001b). The channel and chaos systems demonstrate progressively deeper downcutting and collapse (Witbeck and others, 1991; Rotto and Tanaka, 1995). Some of the earlier discharges of Kasei Valles appear to have originated from the Sacra Fossae troughs (Tanaka and Chapman, 1992). The resultant topography represents the accumulated history of many individual episodes and events, including features related to discharge and recharge, erosion, collapse, deposition, and settling of deposits (Carr, 1979; Nummedal and Prior, 1981; Lucchitta, 1985; MacKinnon and Tanaka, 1989; Harrison and Grimm, 2004; Rodriguez and others, 2005).

EARLY AMAZONIAN EPOCH

The Vastitas Borealis units (ABv_m and ABv_i) generally have been considered to be the result of outflow channel sedimentation (Parker and others, 1989, 1993; Baker and others, 1991; Tanaka, 1997). However, the stratigraphic relations and our crater counts indicate that the Vastitas Borealis units may postdate the youngest Chryse Planitia units (HCc_3 and HCc_4). If an ocean were rapidly emplaced via outflow channel discharges and (or) springs from within the northern plains (as represented by the Hephaestus/Hebrus fracture and valley system, but on a broader scale), it would freeze in approximately 10^4 years and the ice, if it were insulated, would remain in the subsurface (Kreslavsky and Head, 2002). Possibly, such an ice-rich deposit was subsequently reworked perhaps due to one or more significant regional or global warming events and the continued introduction of ground water from aquifers within the substrate and adjacent plains materials. This reworking could have involved deformation, sedimentary volcanism, and (or) mass flow (to explain the lobate edges of the Vastitas Borealis marginal unit) that ultimately might have transformed and augmented a paleo-ocean deposit.

Within the Vastitas Borealis interior unit (ABv_i), the formation of polygonal troughs and circular depressions (also called ghost craters) in Utopia and Acidalia Planitiae and Vastitas Borealis may be related to desiccation, contraction, and relaxation of a water-rich deposit >600 m thick (McGill and Hills, 1992). The polygonal troughs occur mostly in lower elevation areas of the unit within Utopia Planitia and surrounding Planum Boreum. The circular depressions are more widely distributed and likely are buried impact craters whose density indicates that they date at least to the Early Hesperian (Kreslavsky and Head, 2002). Those having double rings in Utopia Planitia suggest that the wet sediment thickness may have been 1 to 2 km (Buczkowski and Cooke, 2004). Alternatively or, perhaps, in addition, polygonal troughs in Utopia Planitia have been proposed to result from rebound after removal of water (Hiesinger and Head, 2000; Thomson and Head, 2001).

Long, sinuous troughs with medial ridges developed in places within the Vastitas Borealis marginal unit (ABv_m). These features have been interpreted variously

as coastal marine spits (Parker and others, 1993), glacial tunnel valleys with eskers (Kargel and others, 1995), and deformation of a partly frozen, wet debris deposit (Tanaka, 1997).

Local regions of the northern lowlands and parts of northwestern Arabia Terra appear to have undergone collapse and other volatile-related landscape modification following formation of the Vastitas Borealis units: (1) Scandia region, which includes Scandia Cavi and other shallower, irregular depressions and scarps north of Scandia Colles and Tantalus Fossae; (2) northern Acidalia Planitia, with irregular depressions and knobby terrains in the Acidalia and Ortygia Colles region; and (3) Cydonia region, including knobby terrain, subtle depressions, and high-standing mesas surrounded by moats in lowland materials and deep pits within highland material. In part, the collapse features may be controlled by ice-rich stratigraphy related to the putative ancient Chryse impact basin (Tanaka, 2004). Collapse is likely due to the removal of subsurface ice. The mesas with moats may represent enhanced pumping of ground water into zones beneath the mesas due to rises in the topography of the permafrost/unfrozen ground interface. The pancake-shaped mesas and irregular hills of Scandia Tholi may represent mud volcanism, perhaps related to pressurization of pore water as the permafrost zone deepened. Alternatively, Fishbaugh and Head (2000) interpreted the features as degraded moraines of a retreated, formerly extensive ice cap.

The troughs of Elysium and Hyblaeus Fossae, which are both concentric with and radial (northwest-trending) to the Elysium rise, cut the Elysium rise unit (AHEe) on the flanks of the rise and served as sources of Tinjar Valles a and b units (AEt_a and AEt_b) and, perhaps, some of the Elysium rise unit as a consequence of magma/ground-ice and water interactions (Mouginis-Mark, 1985; Christiansen, 1989; Tanaka and others, 1992a; Russell and Head, 2003). Possibly associated with this activity, the formation of Hephaestus Fossae and Hebrus Valles in southeastern Utopia Planitia include discontinuous channel scour features originating from depressions and, in some cases, terminating at depressions downslope, as well as pits and polygonal troughs. These features seem to indicate spring discharge of water and both surface and subsurface fluvial erosion along fracture systems. The features originate in Utopia Planitia 2 unit (HBu_2) and dissect the Vastitas Borealis units. East of these features, several scattered patches of elevated, fractured topography indicate sites of possible heaving, perhaps resulting from high pore-volatile pressures.

Some of the major grabens of Tantalus Fossae were reactivated, extending hundreds of kilometers into Vastitas Borealis across Alba Patera, Scandia region, and Vastitas Borealis marginal and interior units (HTa, ABs, ABv_m, and ABv_i). The south contact of the Vastitas Borealis marginal unit rises as much as 650 m above the mean elevation of this contact (~3,800 m) where it crosses Tantalus Fossae, which may be a signature of uplift associated with this region of extension.

Contractional deformation in the Early Amazonian resulted in widely spaced, gently expressed ridges as seen in MOLA data but generally was not detected in Viking and THEMIS images marking the Vastitas Borealis marginal and interior units (ABv_m and ABv_i), Elysium rise unit (AHEe), Chryse Planitia 3 and 4 units (HCc_3 and HCc_4), and surfaces scoured by Kasei and Ares Valles (Tanaka and others, 1991, 2003a). Other Hesperian and Noachian surfaces likely experienced modest Amazonian contraction in places. Most of the ridges in Vastitas Borealis have subdued or symmetric cross-sectional profiles and generally lack crenulations. The subdued forms in Vastitas Borealis may be due to their development in weak surface rocks. Alternatively, Thomson and Head (2001) and Head and others (2002) suggested that the wrinkle ridges in Vastitas Borealis are subdued from mantling by the Vastitas Borealis units and actually are formed only during the Early Hesperian.

The northern plains, especially the Vastitas Borealis units, provide a test area for northern plains cratering analysis because of their apparent uniform age and expansiveness. As mentioned earlier, degraded craters occur within Vastitas Borealis and other older northern plains units. In contrast, younger volcanic materials, including Tinjar Valles and Amazonis Planitia units, do not display the impressions of completely buried craters (fig. 2), which indicates a lack of differential compaction within the volcanic units. The largest crater superposed on the Vastitas Borealis units is the double-ring crater Lyot, with concentric rims about 100 and 200 km in diameter and an Early Amazonian crater density (N(5) = 51±9). It exhibits a few channels dissecting its ejecta. The Vastitas Borealis units display a steep size-frequency distribution of craters such that the N(5) crater density is about ten times that of the N(16) density (table 1), reflecting an ~D^{-2} size-frequency relation. However, Hesperian units such as the Lunae Planum and Utopia Planitia 1 (HNTl and HBu_1) units are consistent with shallower power-law functions (slopes of –1.3 to –1.7). Finally, the Vastitas Borealis interior unit (ABv_i) includes numerous pedestal craters (fig. 2), which indicate that aeolian mantles probably have come and gone within the lower parts of the northern lowlands. These mantles may be related to more active climate regimes and (or) availability of easily mobilized dust.

MIDDLE AMAZONIAN EPOCH

Relatively dense systems of crosscutting, mostly asymmetric ridges developed across Isidis Planitia following formation of the Isidis Planitia unit (AIi) perhaps in response to sediment loading. Like those in Vastitas Borealis, these ridge systems have a subtle topographic

expression. Also, linear, north-trending wrinkle ridges deformed flows of Amazonis Planitia 1 south and north units ($AHAa_{1s}$ and AAa_{1n}). The same system of ridges appears within Amazonis Planitia 2 north unit (AAa_{2n}) and likely is embayed by that unit. Systems of closely spaced fractures (too small to map at this scale), some forming conjugate sets, formed within the Medusae Fossae unit; these features may be eroded tension joints and shear fractures (Tanaka and Golombek, 1989).

Debris aprons of the Deuteronilus Mensae 2 unit (ABd_2) that formed around high-standing mesas of Deuteronilus Mensae display flow structures that indicate ice-lubricated mass flow similar to that of rock glaciers. The ice may have been in the subsurface, indicating that the upper 1 to 2 km of the Noachian materials in this area are ice rich (Mangold and Allemand, 2001). This activity may have begun prior to the Middle Amazonian after the mensae formed in the Late Hesperian and appears to have continued into the Late Amazonian.

The ridge and trough structures of the Olympus Mons aureole material (Lycus Sulci unit, ATl) may have developed as a result of landsliding or gravity spreading of the lower flanks of the Olympus Mons shield (Lopes and others, 1980; Francis and Wadge, 1983; Tanaka, 1985; McGovern and others, 2004).

The Scandia region unit (ABs) is deeply eroded; much of the erosion occurred sometime between unit emplacement in the Early Amazonian and its mantling by Planum Boreum 1 and 2 units (ABb_1 and ABb_2) in the Late Amazonian. This erosion, which appears to be ongoing, produces the dark dunes of the Olympia Undae unit (ABo; Malin and Edgett, 2001; Byrne and Murray, 2002; Wyatt and others, 2004; Fishbaugh and Head, 2005)

LATE AMAZONIAN EPOCH

In southern Amazonis Planitia, a conjugate system of northeast-trending scarps and northwest-trending ridges deform the Amazonis Planitia 2 south and Arcadia Planitia units (AAa_{2s} and HAa) and may be strike-slip faults and contractional wrinkle ridges, respectively (Tanaka and others, 2003b). Cerberus Fossae propagated through the Elysium rise unit (AHEe), as both aqueous floods and lavas were discharged from some locations along the fracture system (Burr and others, 2002a,b).

The Scandia region and the Planum Boreum 1 and 2 units (ABs, ABb_1, and ABb_2) making up Planum Boreum underwent significant erosion, resulting in local, steep scarps. Some investigators proposed that glacial-like flow of Planum Boreum (Clifford, 1987; Fisher, 2000) and subglacial melt-water discharges from beneath Planum Boreum (Dial and Dohm, 1994; Benito and others, 1997; Fishbaugh and Head, 2002) created this topography, but others suggest that such processes did not occur (Kolb and Tanaka, 2001; Malin and Edgett, 2001).

GEOLOGIC SYNTHESIS

The geologic history of the northern plains of Mars based on this geologic map must be regarded as provisional and interpretive, given uncertainties in rock compositions and formational processes, character and timing of landform modification, and unit and feature associations.

PRE-NOACHIAN AND NOACHIAN

The northern plains basin formed by impact and (or) tectonic processes during heavy bombardment following the solidification of the planet's crust. Next, large impacts produced quasi-circular depressions, including Utopia basin, in crustal rocks underlying the oldest exposed Noachian rocks. During the Noachian, waning bombardment produced impact structures, including Isidis basin, in surface rocks. Noachian rocks include a mixture of impact breccia and melt, volcanic rocks, and clastic sedimentary rocks of aeolian, alluvial, mass-wasting, and other undetermined origins. The impacted crust developed a porous, fractured, and poorly sorted megaregolith in which ices and liquids were emplaced by various means. Much of the volcanic and possibly intrusive build-up of the broad Tharsis rise took place. Large impacts and early tectonism, perhaps Tharsis related, resulted in local uplifts and formation of massifs. Relaxation of the lithosphere surrounding the Isidis impact led to development of Nili Fossae, and rifting radial to Syria Planum (outside of the map area) produced Tempe Fossae. Planetary cooling resulted in contractional deformation in most areas. Toward the end of the Noachian, sapping and surface runoff produced valley networks, likely fed by precipitation of rain and (or) snow and, perhaps, sustained by hydrothermal activity. Along the highland/lowland boundary and across the Elysium-Arcadia-Amazonis plains, wholesale mass-wasting and subsurface volatile movements led to fracturing, collapse, disintegration of Noachian rocks into mesas and knobs, and emplacement of mass flows and plains deposits. Potentially, significant dissection along outflow channels and highland valleys from the Tharsis rise and northwestern Arabia Terra may have occurred at this time, but evidence for this is obscure due to later resurfacing.

HESPERIAN

Volcanic buildup of the Tharsis rise, formation of Tempe Fossae, widespread contractional deformation, and highland boundary degradation continued from the Noachian into the Hesperian. Volcanism also led to development of the Elysium rise, Syrtis Major Planum, and emplacement of lava flows throughout much of Arcadia and Amazonis Planitiae, generally after initial highland boundary degradation ceased. During the Late Hesperian, an episode of widespread erosion of the high-

land boundary resulted in (1) collapse and mass-wasting of Early Hesperian lowland and Noachian highland material along margins of Utopia, Isidis, and Elysium Planitiae, (2) fretted terrain formation in the Deuteronilus Mensae region, and (3) outflow channel dissection and chaos development on the eastern flank of the Tharsis rise and across Margaritifer Terra and Chryse Planitia. Each of these erosional processes likely involved large amounts of water and, perhaps, some carbon dioxide to enable collapse, disintegration, and transport of surface materials; also, magmatic and impact events may have triggered the activity. Details of the development of outflow channel and chaotic terrain are uncertain, because much of the evidence for earlier phases of activity likely has been destroyed or buried by younger activity.

AMAZONIAN

The Amazonian began with formation of the Vastitas Borealis units. The exposed margin of the units is at relatively constant elevation, supporting the hypothesis that the units resulted from emplacement within a body of water. Because the Vastitas Borealis units embay the Chryse channel system and Acidalia Mensa at low elevation within Acidalia Planitia and have a lower crater density than Chryse Planitia units, the Vastitas Borealis units may have resulted from periglacial reworking of plains deposits and (or) spring discharges from within the northern plains, rather than or in addition to outflow-channel discharges. Such activity produced marginal and interior trough and pitted cone features, as well as collapse features, in Acidalia and Cydonia and in the Scandia region unit. Fine particles produced by weathering and erosion of the Scandia region and Vastitas Borealis units and, perhaps, other materials led to the formation of dispersed pedestal craters, an extant mantle in northwestern Utopia Planitia, and the basal platform of Planum Boreum. Renewed volcanism at Syrtis Major Planum may have been responsible for the generation of material covering Isidis Planitia, which underwent reworking and contractional deformation similar to that seen in the Vastitas Borealis units.

The graben formation at Tantalus Fossae and the impact of Lyot crater deeply fractured the crust along the highland/lowland boundary without significant associated volatile discharges. However, discharges on the west flank of the Elysium rise led to collapse, which formed Elysium Fossae, carved channels, and deposited volcaniclastic flows in Utopia Planitia. Likely, magma/volatile interactions were involved. Shield volcanism waned on the Tharsis and Elysium rises, but large flow fields were emplaced onto adjacent Utopia, Elysium, and Amazonis Planitiae in separate pulses of activity. Episodic discharges from fracture-controlled depressions in the lowlands surrounding the Elysium rise carved lower Hephaestus Fossae, Hebrus Valles, Marte Vallis, and other channel systems near Cerberus Fossae. Along the south margin of Elysium Planitia, the Medusae Fossae unit underwent deformation and reworking, perhaps related to near-surface volatile activity. Ice- and possibly water-lubricated slope movements formed the Olympus Mons aureole deposits and debris aprons in the Deuteronilus Mensae region. Some of the youngest fluvial discharges on Mars, perhaps just millions of years old, originated from Cerberus Fossae and coincided with pulses of volcanism from the fossae and nearby vents. Additional, young lava flows erupted from vents in southeastern Amazonis Planitia and were subsequently faulted by conjugate contractional and, possibly, strike-slip structures. Erosion of dark basal material of Planum Boreum formed the dark, circumpolar dunes. Water ice and dust were rhythmically layered atop Planum Boreum, accumulating to hundreds of meters and more in thickness, and were subsequently eroded over the past few millions of years. Several additional layers of dust and the residual ice cap that may represent polar dust and ice deposition during the past few million years now coat much of Planum Boreum and patches of surrounding terrain.

ACKNOWLEDGMENTS

We wish to thank Mary Chapman (U.S. Geological Survey) and Taylor Joyal and Alisa Wenker (Northern Arizona University) for assistance with preliminary geologic mapping of the study region. Jenny Blue (U.S. Geological Survey) and the Mars Task Group of the Working Group for Planetary System Nomenclature (International Astronomical Union) helped with updating geographic nomenclature to adapt to new topographic and image observations. Nadine Barlow (Northern Arizona University) provided updated versions of her Mars crater database to assist with our crater counting. James Dohm (University of Arizona) and Leslie Bleamaster (Planetary Science Institute) provided insightful comments that improved, in particular, the map text. Jan Zigler (U.S. Geological Survey) edited the map and helped us incorporate format and style standards used in terrestrial geologic maps.

REFERENCES CITED

Albee, A.L., Arvidson, R.E., Palluconi, F.D., Thorpe, T.E., 2001, Overview of the Mars Global Surveyor mission: Journal of Geophysical Research, v. 106, no. E10, p. 23,291–23,316.

Baker, V.R., Maruyama, Shigenori, and Dohm, J.M., 2002, A theory of early plate tectonics and subsequent long-term superplume activity on Mars: Electronic Geosciences, v. 7.

Baker, V.R., and Milton, D.J., 1974, Erosion by catastrophic floods on Mars and Earth: Icarus, v. 23, p. 27–41.

Baker, V.R., Strom, R.G., Gulick, V.C., Kargel, J.S., Komatsu, Goro, and Kale, V.S., 1991, Ancient oceans, ice sheets, and the hydrological cycle on Mars: Nature, v. 352, p. 589–594.

Bandfield, J.L., Hamilton, V.E., and Christensen, P.R., 2000, A global view of Martian surface compositions from MGS-TES: Science, v. 287, p. 1626–1630.

Barlow, N.G., 1988, Crater size-frequency distributions and a revised Martian relative chronology: Icarus, v. 75, p. 285–305.

Barlow, N.G., Koroshetz, John, and Dohm, J.M., 2001, Variations in the onset diameter for Martian layered ejecta morphologies and their implications for subsurface volatile reservoirs: Geophysical Research Letters, v. 28, p. 3095–3099.

Benito, G., Mediavilla, M., Fernandez, A., Marquez, A., Martinez, J., and Anquita, F., 1997, Chasma Boreale, Mars—A sapping and outflow channel with a tectono-thermal origin: Icarus, v. 129, p. 528–538.

Blasius, K.R., Cutts, J.A., and Howard, A.D., 1982, Topography and stratigraphy of Martian polar layered deposits: Icarus, v. 50, p. 140–160.

Breed, C.S., Grolier, M.J., and McCauley, J.F., 1979, Morphology and distribution of common "sand" dunes on Mars—Comparison with the Earth: Journal of Geophysical Research, v. 84, p. 8183–8204.

Buczkowski, D.L., and Cooke, M.L., 2004, Formation of double-ring circular grabens due to volumetric compaction over buried impact craters—Implications for thickness and nature of cover material in Utopia Planitia, Mars: Journal of Geophysical Research, v. 109, p. 1–8 (doc. no. E02006, doi:10.1029/2003JE002144).

Burr, D.M., Grier, J.A., McEwen, A.S., and Keszthelyi, L.P., 2002a, Repeated aqueous flooding from the Cerberus Fossae—Evidence for very recently extant, deep groundwater on Mars: Icarus, v. 159, p. 53–73.

Burr, D.M., McEwen, A.S., and Sakimoto, S.E.H., 2002b, Recent aqueous floods from the Cerberus Fossae, Mars: Geophysical Research Letters, v. 29, no. 1, p. 13-1 to 13-8 (doi:10.1029/2001GL013345).

Byrne, Shane, and Murray, B.C., 2002, North polar stratigraphy and the paleo-erg of Mars: Journal of Geophysical Research, v. 107, no. E6, p. 11-1 to 11-12 (doc. no. 5044, doi:10.1029/2001JE001615).

Carr, M.H., 1979, Formation of Martian flood features by release of water from confined aquifers: Journal of Geophysical Research, v. 84, p. 2995–3007.

———1986, Mars—A water-rich planet?: Icarus, v. 68, p. 187–216.

Carr, M.H., and Clow, G.D., 1981, Martian channels and valleys—Their characteristics, distribution, and age: Icarus, v. 48, p. 91–117.

Carr, M.H., and Head, J.W., III, 2003, Oceans on Mars—An assessment of the observational evidence and possible fate: Journal of Geophysical Research, v. 108, no. E5, p. 8-1 to 8-28 (doc. no. 5042, doi:10.1029/2002JE001963).

Carr, M.H., and Malin, M.C., 2000, Meter-scale characteristics of Martian channels and valleys: Icarus, v. 146, p. 366–386.

Carruthers, M.W., and McGill, G.E., 1998, Evidence for igneous activity and implications for the origin of a fretted channel in southern Ismenius Lacus, Mars: Journal of Geophysical Research, v. 103, p. 31,433–31,443.

Christensen, P.R., Morris, R.V., Lane, M.D., Bandfield, J.L., and Malin, M.C., 2001, Global mapping of Martian hematite mineral deposits—Remnants of water-driven processes on early Mars: Journal of Geophysical Research, v. 106, p. 23,873–23,885.

Christiansen, E.H., 1989, Lahars in the Elysium region of Mars, Geology, v. 17, p. 203–206.

Clifford, S.M., 1987, Polar basal melting on Mars: Journal of Geophysical Research, v. 92, p. 9135–9152.

Clifford, S.M., and Parker, T.J., 2001, The evolution of the Martian hydrosphere—Implications for the fate of a primordial ocean and the current state of the northern plains: Icarus, v. 154, p. 40–79.

Costard, F.M., and Kargel, J.S., 1995, Outwash plains and thermokarst on Mars: Icarus, v. 114, p. 93–112.

Craddock, R.A., and, Howard, A.D., 2002, The case for rainfall on a warm, wet early Mars: Journal of Geophysical Research, v. 107, no. E11, p. 21-1 to 21-25 (doc no. 5111, doi:10.1029/2001JE001505).

Craddock, R.A., and Maxwell, T.A., 1993, Geomorphic evolution of the Martian highlands through ancient fluvial processes: Journal of Geophysical Research, v. 98, p. 3453–3468.

Crumpler, L.S., Craddock, R.A., and Aubele, J.C., 2001, Geologic map of the MTM 25047 and 20047 quadrangles, central Chryse Planitia/Viking 1 Lander site, Mars: U.S. Geological Survey Geologic Investigations Series I–2693, scale 1:1,000,000 [available on World Wide Web at http://geopubs.wr.usgs.gov/i-map/i2693].

Crumpler, L.S., and Tanaka, K.L., 2003, Geology and MER target site characteristics along the southern rim of Isidis Planitia, Mars: Journal of Geophysical Research, v. 108, no. E12, p. ROV 21-1 to ROV 21-42 (doc. no. 8080, doi:10.1029/2002E002040).

Cutts, J.A., 1973, Nature and origin of layered deposits of the Martian polar regions: Journal of Geophysical Research, v. 78, p. 4231–4249.

Dial, A.L., Jr., 1984, Geologic map of the Mare Boreum area of Mars: U.S. Geological Survey Miscellaneous Investigations Series Map I–1640, scale 1:5,000,000.

Dial, A.L., and Dohm, J.M., 1994, Geologic map of science study area 4, Chasma Boreale region of Mars: U.S. Geological Survey Miscellaneous Investigations Series Map I–2357, scale 1:500,000.

Dohm, J.M., Anderson, R.C., Baker, V.C., and 8 others, 2001a, Latent outflow activity for western Tharsis, Mars—Significant flood record exposed: Journal of Geophysical Research, v. 106, p. 12,301–12,314.

Dohm, J.M., Ferris, J.C., Baker, V.R., Anderson, R.C., Hare, T.M., Strom, R.G., Barlow, N.G., Tanaka, K.L., Klemaszewski, J.E., and Scott, D.H., 2001b, Ancient drainage basin of the Tharsis region, Mars—Potential source for outflow channel systems and putative oceans or paleolakes: Journal of Geophysical Research, v. 106, p. 32,943–32,958.

Fairén, A.G., and Dohm, J.M., 2004, Age and origin of the lowlands of Mars: Icarus, v. 168, p. 277–284.

Fairén, A.G., Dohm, J.M., Baker, V.R., de Pablo, M.A., Ruiz, Javier, Ferris, J.C., and Anderson, R.C., 2003, Episodic flood inundations of the northern plains of Mars: Icarus, v. 165, p. 53–67.

Fishbaugh, K.E., and Head, J.W., III, 2000, North polar region of Mars—Topography of circumpolar deposits from Mars Orbiter Laser Altimeter (MOLA) data and evidence for asymmetric retreat of the polar cap: Journal of Geophysical Research, v. 105, p. 22,455–22,486.

———2001, Comparison of the north and south polar caps of Mars—New observations from MOLA data and discussion of some outstanding questions: Icarus, v. 154, p. 145–161.

———2002, Chasma Boreale, Mars—Topographic characterization from Mars Orbiter Laser Altimeter data and implications for mechanisms of formation: Journal of Geophysical Research, v. 107, no. E3, p. 2-1 to 2-26 (doi:10.1029/2000JE001351).

———2005, Origin and characteristics of the Mars north polar basal unit and implications for polar geologic history: Icarus, v. 174, p. 444–474.

Fisher, D.A., 2000, Internal layers in an "accublation" ice cap—A test for flow: Icarus, v. 144, p. 289–294.

Francis, P.W., and Wadge, Geoff, 1983, The Olympus Mons aureole—Formation by gravitational spreading: Journal of Geophysical Research, v. 88, p. 8333–8344.

Frey, H.V., 2004, A timescale for major events in early Mars crustal evolution [abs.], *in* Lunar and Planetary Science Conference, 35th, March 13–19, 2004: Houston, Tex., Lunar and Planetary Institute, no. 3104 [CD-ROM].

Frey, H.V., and Jarosewich, Martha, 1982, Subkilometer Martian volcanoes—Properties and possible terrestrial analogs: Journal of Geophysical Research, v. 87, p. 9867–9879.

Frey, H.V., Roark, J.H., Shockey, K.M., Frey, E.L., and Sakimoto, S.E.H., 2002, Ancient lowlands on Mars: Geophysical Research Letters, v. 29, no. 10, p. 22-1 to 22-4 (doi:10.1029/2001GL013832).

Frey, H.V., and Schultz, R.A., 1988, Large impact basins and the mega-impact origin for the crustal dichotomy of Mars: Geophysical Research Letters, v. 15, no. 3, p. 229–232.

Fuller, R.R., and Head, J.W., III, 2002, Amazonis Planitia—The role of geologically recent volcanism and sedimentation in the formation of the smoothest plains on Mars: Journal of Geophysical Research, v. 107, no. E10, p. 11-1 to 11-25 (doc. no. 5081, doi:10.1029/2002JE001842).

———2003, Olympus Mons, Mars—Detection of extensive preaureole volcanism and implications for initial mantle plume behavior: Geology, v. 31, no. 2, p. 175–178.

Garvin, J.B., Sakimoto, S.E.H., Frawley, J.J., Schnetzler, C.C., and Wright, H.M., 2000, Topographic evidence for geologically recent near-polar volcanism on Mars: Icarus, v. 145, 648–652.

Greeley, Ronald, and Guest, J.E., 1987, Geologic map of the eastern equatorial region of Mars: U.S. Geological Survey Miscellaneous Investigations Series Map I–1802–B, scale 1:15,000,000.

Grizzaffi, Patricia, and Schultz, P.H., 1989, Isidis basin—Site of ancient volatile-rich debris layer: Icarus, v. 77, p. 358–381.

Hansen, V.L., 2000, Geologic mapping of tectonic planets—Earth and Planetary Science Letters, v. 176, p. 527–542.

Harrison, K.P., and Grimm, R.E., 2004, Tharsis recharge—A source of water for martian outflow channels: Geophysical Research Letters, v. 31, p. 1–4 (doc. no. L14703, doi:10.1029/2004GL020502).

Hartmann, W.K., and Neukum, Gerhard, 2001, Cratering chronology and the evolution of Mars: Space Science Reviews, v. 96, p. 165–194.

Head, J.W., III, Hiesinger, Harald, Ivanov, M.I., Kreslavsky, M.A., Pratt, Stephen, and Thomson, B.J., 1999, Possible ancient oceans on Mars—Evidence from Mars Orbiter Laser Altimeter data: Science, v. 286, p. 2134–2137.

Head, J.W., III, Kreslavsky, M.A., and Pratt, Stephen, 2002, Northern lowlands of Mars—Evidence for widespread volcanic flooding and tectonic deformation in the Hesperian Period: Journal of Geophysical Research, v. 107, no. E1, p. 3-1 to 3-29 (doi:10.1029/2000JE001445).

Head, J.W., Mustard, J.F., Kreslavsky, M.A., Millikan, R.E., and Marchant, D.R., 2003, Recent ice ages on Mars: Nature, v. 426, p. 797–802.

Herkenhoff, K.E., and Plaut, J.J., 2000, Surface ages and resurfacing rates of the polar layered deposits on Mars: Icarus, v. 144, p. 243–253.

Hiesinger, Harald, and Head, J.W., III, 2000, Characteristics and origin of the polygonal terrain in southern Utopia Planitia, Mars—Results from Mars Orbiter Laser Altimeter and Mars Orbiter Camera data: Journal of Geophysical Research, v. 105, p. 11,999–12,022.

———2004, The Syrtis Major volcanic province, Mars—Synthesis from Mars Global Surveyor data: Journal of Geophysical Research, v. 109, p. 1–37 (doc no. E01004, doi:10.1029/2003JE002143).

Hoffman, Nick, 2000, White Mars—A new model for Mars' surface and atmosphere based on CO_2: Icarus, v. 146, p. 326–342.

Howard, A.D., 1978, Origin of the stepped topography of the Martian poles: Icarus, v. 34, p. 581–599.

Howard, A.D., Cutts, J.A., and Blasius, K.R., 1982, Stratigraphic relationships within Martian polar-cap deposits: Icarus, v. 50, p. 161–215.

Hynek, B.M., and Phillips, R.J., 2001, Evidence for extensive denudation of the Martian highlands: Geology, v. 29, p. 407–410.

———2003, New data reveal mature, integrated drainage systems on Mars indicative of past precipitation: Geology, v. 31, p. 757–760.

Hynek, B.M., Phillips, R.J., and Arvidson, R.E., 2003, Explosive volcanism in the Tharsis region—Global evidence in the Martian geologic record: Journal of Geophysical Research, v. 108, no. E9, p. 15-1 to 15-16 (doc. no. 5111, doi:10.1029/2003JE002062).

Irwin, R.P., Maxwell, T.A., Howard, A.D., Craddock, R.A., and Leverington, D.W., 2002, A large paleolake basin at the head of Ma'adim Vallis, Mars: Science, v. 296, p. 2209–2212.

Ivanov, M.A., and Head, J.W., III, 2003, Syrtis Major and Isidis Basin contact—Morphological and topographic characteristics of Syrtis Major lava flows and material of the Vastitas Borealis Formation: Journal of Geophysical Research, v. 108, no. E6, p. 17-1 to 17-23 (doc. no. 5063, doi:10.1029/2002JE001994).

Kargel, J.S., Baker, V.R., Begét, J.E., Lockwood, J.F., Péwé, T.L., Shaw, J.S., and Strom, R.G., 1995, Evidence of ancient continental glaciation in the Martian northern plains: Journal of Geophysical Research, v. 100, no. E3, p. 5351–5368.

Kargel, J.S., and Strom, R.G., 1992, Ancient glaciation on Mars: Geology, v. 20, p. 3–7.

Keszthelyi, Laszlo, McEwen, A.S., and Thordarson, T., 2000, Terrestrial analogs and thermal models for Martian flood lavas: Journal of Geophysical Research, v. 105, p. 15,027–15,050.

Kolb, E.J., and Tanaka, K.L., 2001, Geologic history of the polar regions of Mars based on Mars Global Surveyor data—II. Amazonian Period: Icarus, v. 154, p. 22–39.

Koutnik, Michelle, Byrne, Shane, and Murray, B.C., 2002, South Polar Layered Deposits of Mars—The cratering record: Journal of Geophysical Research, v. 107, no. E11, p. 10-1 to 10-10 (doc. no. 5100, doi:10.1029/2001JE001805).

Kreslavsky, M.A., and Head, J.W., III, 2000, Kilometer-scale roughness of Mars—Results from MOLA data analysis: Journal of Geophysical Research, v. 105, no. E11, p. 26,695–26,711.

———2002, Fate of outflow channel effluents in the northern lowlands of Mars—The Vastitas Borealis Formation as a sublimation residue from frozen ponded bodies of water: Journal of Geophysical Research, v. 107, no. E12, p. 4-1 to 4-25 (doc. no. 5121, doi:10.1029/2001JE001831).

Lanagan, P.D., 2004, Geologic history of the Cerberus Plains, Mars: Tucson, University of Arizona, Ph.D. dissertation, 142 p.

Lancaster, Nicholas, and Greeley, Ronald, 1990, Sediment volume in the north polar sand seas of Mars: Journal of Geophysical Research, v. 95, no. B7, p. 10,921–10,927.

Laskar, Jacques, Levrard, Benjamin, and Mustard, J.F., 2002, Orbital forcing of the martian polar layered deposits: Nature, v. 419, p. 375–377.

Lopes, R.M.C., Guest, J.E., and Wilson, C.J., 1980, Origin of the Olympus Mons aureole and perimeter scarp—The Moon and the Planets, v. 22, p. 221–234.

Lucchitta, B.K., 1981, Mars and Earth—Comparison of cold-climate features: Icarus, v. 45, p. 264–303.

———1982, Ice sculpture in the Martian outflow channels: Journal of Geophysical Research, v. 87, no. B12, p. 9951–9973.

———1984, Ice and debris in the fretted terrain, Mars, *in* Proceedings of the Lunar and Planetary Science Conference, 14th, February, 1984: Journal of Geophysical Research, v. 89, pt. 2, supplement, p. B409–B418.

———1985, Geomorphologic evidence from ground ice on Mars, *in* Klinger, J., Benest, D., Dollfus, A and others (eds.), Ices in the Solar System: Dordrecht, Holland, D. Reidel Publishing Co., p. 583–604.

Lucchitta, B.K., Ferguson, H.M., and Summers, Cathy, 1986, Sedimentary deposits in the northern lowland plains, Mars, *in* Proceedings of the Lunar and Planetary Science Conference, 17th, Part 1, November, 1986: Journal of Geophysical Research, v. 91, supplement, no. B13, p. E166–E174.

MacKinnon, D.J., and Tanaka, K.L., 1989, The impacted Martian crust—Structure, hydrology, and some geologic implications: Journal of Geophysical Research, v. 94, no. B12, p. 17,359–17,370.

Malin, M.C., and Edgett, K.S., 2001, Mars Global Surveyor Mars Orbiter Camera—Interplanetary cruise through primary mission: Journal of Geophysical Research, v. 106, no. E10, p. 23,429–23,570.

———2005, MGS MOC—First views of Mars at submeter resolution from orbit [abs.], *in* Lunar and Planetary Science Conference, 36th, March 14–18, 2005: Houston, Tex., Lunar and Planetary Institute, no. 1172 [CD-ROM].

Mangold, N., and Allemand, P., 2001, Topographic analysis of features related to ice on Mars: Geophysical Research Letters, v. 28, no. 3, p. 407–410.

Mangold, N., Allemand, P., Duval, P., Geraud, Y., and Thomas, P., 2002, Experimental and theoretical deformation of ice-rock mixtures—Implications on rheology and ice content of Martian permafrost: Planetary and Space Science, v. 50, p. 385–401.

Mangold, N., Maurice, S., Feldman, W.C., Costard, F., and Forget, F., 2004, Spatial relationships between patterned gound and ground ice detected by the Neutron Spectrometer on Mars: Journal of Geophysical Research, v. 109, p. 1–6 (doc. no. E08001, doi:10.1029/2004JE002235).

McBride, S.A., Allen, C.C., and Bell, M.S., 2005, Prospecting for Martian ice [abs.], *in* Lunar and Planetary Science Conference, 36th, March 14–18, 2005: Houston, Tex., Lunar and Planetary Institute, no. 1090 [CD-ROM].

McEwen, A.S., Malin, M.C., Carr, M.H., and Hartmann, W.K., 1999, Voluminous volcanism on early Mars revealed in Valles Marineris: Nature, v. 397, p. 584–86.

McEwen, A.S., Preblich, B.S., Turtle, E.P., and 6 others, 2005, The rayed crater Zunil and interpretations of small impact craters on Mars: Icarus, v. 176, p. 351–381..

McGill, G.E., 1989, Buried topography of Utopia, Mars—Persistence of a giant impact depression: Journal of Geophysical Research, v. 94, no. B3, p. 2753–2759.

———2000, Crustal history of north central Arabia Terra, Mars: Journal of Geophysical Research, v. 105, p. 6945–6959.

———2002, Geologic map transecting the highland/lowland boundary zone, Arabia Terra, Mars—Quadrangles 30332, 35332, 40332, and 45332: U.S. Geological Survey Geologic Investigations Series I–2746, scale 1:1,000,000 [available on World Wide Web at http://geopubs.wr.usgs.gov/i-map/i2746].

McGill, G.E., and Hills, L.S., 1992, Origin of giant Martian polygons: Journal of Geophysical Research, v. 97, p. 2633–2647.

McGovern, P.J., Smith, J.R., Morgan, J.K., and Bulmer, M.H., 2004, The Olympus Mons aureole deposits—New evidence for a flank-failure origin: Journal of Geophysical Research, v. 109, p. 1–10 (doc. no: E08008, doi:10.1029/2004JE002258).

Michalski, J.R., Kraft, M.D., Sharp, T.G., Williams, L.B., and Christensen, P.R., 2005, Mineralogical constraints on the high-silica martian surface component observed by TES: Icarus, v. 174, no. 1, p. 161–177.

Moore, H.J., 2001, Geologic map of the Tempe-Mareotis region of Mars: U.S. Geological Survey Geologic Investigations Series I–2727, scale 1:1,000,000 [available on World Wide Web at http://geopubs.wr.usgs.gov/i-map/i2727].

Morris, E.M., and Tanaka, K.L., 1994, Geologic maps of the Olympus Mons region of Mars: U.S. Geological Survey Miscellaneous Investigations Series Map I–2327, scales 1:2,000,000 and 1:1,000,000.

Mouginis-Mark, P.J., 1985, Volcano/ground ice interactions in Elysium Planitia, Mars: Icarus, v. 64, p. 265–282.

Murray, B.C., Soderblom, L.A., Cutts, J.A., Sharp, R.P., Milton, D.J., and Leighton, R.B., 1972, Geological framework of the south polar region of Mars: Icarus, v. 17, p. 328–345.

Mustard, J.F., Cooper, C.D., and Rifkin, M.K., 2001, Evidence for recent climate change on Mars from the identification of youthful near-surface ground ice: Nature, v. 412, p. 411–414.

Neumann, G.A., Rowlands, D.D., Lemoine, F.G., Smith, D.E., and Zuber, M.T., 2001, Crossover analysis of Mars Orbiter Laser Altimeter data: Journal of Geophysical Research, v. 106, no. E10, p. 23,753–23,768.

Nimmo, Francis, and Tanaka, K.L., 2005, Early crustal evolution of Mars: Annual Review of Earth and Planetary Sciences, v. 33, p. 133–161.

North American Commission on Stratigraphic Nomenclature, 1983, North American stratigraphic code: American Association of Petroleum Geologists Bulletin, v. 67, no. 5, p. 841–875.

Nummedal, Dag, and Prior, D.B., 1981, Generation of Martian chaos and channels by debris flows: Icarus, v. 45, p. 77–86.

Parker, T.J., Gorsline, D.S., Saunders, R.S., Pieri, D.C., and Schneeberger, D.M., 1993, Coastal geomorphology of the Martian northern plains: Journal of Geophysical Research, v. 98, no. E6, p. 11,061–11,078.

Parker, T.J., Saunders, R.S., and Schneeberger, D.M., 1989, Transitional morphology in west Deuteronilus Mensae, Mars: Implications for modification of the lowland/upland boundary: Icarus, v. 82, p. 111–145.

Plescia, J.B., 2003, Cerberus Fossae, Elysium, Mars—A source for lava and water: Icarus, v. 164, p. 79–95.

Rodriguez, J.A.P., Sasaki, Sho, Dohm, J.M., and 10 others, in press, Control of impact crater fracture systems on subsurface hydrology, ground subsidence and collapse, Mars: Journal of Geophysical Research, v. 110, p. 1–22 (doc. no. E06003, doi:10.1029/2004JE002365).

Rogers, A.D., Christensen, P.R., and Bandfield, J.L., 2005, Compositional heterogeneity of the ancient martian crust—Analysis of Ares Vallis bedrock with THEMIS and TES data: Journal of Geophysical Research, v. 110, p. 1–26 (doc no. E05010, doi:10.1029/2005JE00234).

Rossbacher, L.A., and Judson, Sheldon, 1981, Ground ice on Mars—Inventory, distribution, and resulting landforms: Icarus, v. 45, p. 39–59.

Rotto, Sue, and Tanaka, K.L., 1995, Geologic/geomorphic map of the Chryse Planitia region of Mars: U.S.

Geological Survey Miscellaneous Investigations Series Map I–2441, scale 1:5,000,000.

Russell, P.S., and Head, J.W., 2003, Elysium-Utopia flows as mega-lahars—A model of dike intrusion, cryosphere cracking, and water-sediment release: Journal of Geophysical Research, v. 108, no. E6, p. 18-1 to 18-28 (doc. no. 5064, doi:10.1029/2002JE001995).

Salvatore, Amos, ed., 1994, International stratigraphic guide—A guide to stratigraphic classification, terminology, and procedure (2nd ed.): Boulder, Colo., The Geological Society of America, Inc., 214 p.

Schultz, P.H., Schultz, R.A., and Rogers, John, 1982, The structure and evolution of ancient impact basins on Mars: Journal of Geophysical Research, v. 87, no. B12, p. 9803–9820.

Scott, D.H., 1991, Geologic map of MTM quadrangles 25057 and 25052, Kasei Valles region of Mars: U.S. Geological Survey Miscellaneous Investigations Series Map I–2208, scale 1:500,000.

Scott, D.H., and Carr, M.H., 1978, Geologic map of Mars: U.S. Geological Survey Miscellaneous Investigations Series Map I–1083, scale 1:25,000,000.

Scott, D.H., and Dohm, J.M., 1990, Faults and ridges—Historical development in Tempe Terra and Ulysses Patera regions of Mars, *in* Lunar and Planetary Science Conference, Proceedings, 1990: Houston, Tex., Lunar and Planetary Institute, v. 20, p. 503–513.

Scott, D.H., Dohm, J.M., and Rice, J.W., Jr., 1995, Map of Mars showing channels and possible paleolake basins: U.S. Geological Survey Miscellaneous Investigations Series Map I–2461, scale 1:30,000,000.

Scott, D.H., and Tanaka, K.L., 1982, Ignimbrites of Amazonis Planitia region of Mars: Journal of Geophysical Research, v. 87, no. B2, p. 1179–1190.

———1986, Geologic map of the western equatorial region of Mars: U.S. Geological Survey Miscellaneous Investigations Series Map I–1802–A, scale 1:15,000,000.

Scott, D.H., and Underwood, J.R., Jr., 1991, Mottled terrain—A continuing Martian enigma, *in* Lunar and Planetary Science Conference, Proceedings, 1991: Houston, Tex., Lunar and Planetary Institute, v. 21, p. 627–634.

Seidelmann, P.K., Abalakin, V.K., Bursa, M., Davies, M.E., De Bergh, C., Lieske, J.H., Oberst, J., Simon, J.L., Standish, E.M., Stooke, P.J., and Thomas, P.C., 2002, Report of the IAU/IAG Working Group on Cartographic Coordinates and Rotational Elements of the Planets and Satellites—2000: Celestial Mechanics and Dynamical Astronomy, v. 82, p. 83–110.

Sharp, R.P., 1973, Mars—Fretted and chaotic terrains: Journal of Geophysical Research, v. 78, no. 20, p. 4073-4083.

Smith, D.E., Zuber, M.T., Frey, H.V., and 21 others, 2001, Mars Orbiter Laser Altimeter—Experiment summary after the first year of global mapping of Mars: Journal of Geophysical Research, v. 106, no. E10, p. 23,689–23,722.

Smith, D.E., Zuber, M.T., Solomon, S.C., and 16 others, 1999, The global topography of Mars and implications for surface evolution: Science, v. 284, p. 1495–1503.

Squyres, S.W., 1978, Martian fretted terrain—Flow of erosional debris: Icarus, v. 34, p. 600–613.

———1979a, The distribution of lobate debris aprons and similar flows on Mars: Journal of Geophysical Research, v. 84, p. 8087–8096.

———1979b, The evolution of dust deposits in the Martian north polar region: Icarus, v. 40, p. 244–261.

Tanaka, K.L., 1985, Ice-lubricated gravity spreading of the Olympus Mons aureole deposits: Icarus, v. 62, p. 191–206.

———1986, The stratigraphy of Mars, *in* Proceedings of the Lunar and Planetary Science Conference, 17th, Part 1, November, 1986: Journal of Geophysical Research, v. 91, supplement, no. B13, p. E139–158.

———1990, Tectonic history of the Alba Patera-Ceraunius Fossae region of Mars, *in* Lunar and Planetary Science Conference, Proceedings, 1990: Houston, Tex., Lunar and Planetary Institute, v. 20, p. 515–523.

———1997, Sedimentary history and mass flow structures of Chryse and Acidalia Planitiae, Mars: Journal of Geophysical Research, v. 102, p. 4131–4150.

———1999, Debris-flow origin for the Simud/Tiu deposit on Mars: Journal of Geophysical Research, v. 104, p. 8637–8652.

———2000, Dust and ice deposition in the Martian geologic record: Icarus, v. 144, p. 254–266.

———2004, Topographic and geomorphic modification history of the highland/lowland dichotomy boundary of Mars—II. Hesperian and Amazonian Periods [abs.], in Workshop on Hemispheres Apart—The Origin and Modification of the Martian Crustal Dichotomy, Houston, Tex., Sept. 30–Oct. 1, 2004: Houston, Tex., Lunar and Planetary Institute, no. 4030.

Tanaka, K.L., Carr, M.H., Skinner, J.A., Gilmore, M.S., and Hare, T.M., 2003a, Geology of the MER 2003 "Elysium" candidate landing site in southeastern Utopia Planitia, Mars: Journal of Geophysical Research, v. 108, no. E12, p. ROV 20-1 to ROV 20-19 (doc. no: 8079, doi:10.1029/2003JE002054).

Tanaka, K.L., and Chapman, M.G., 1990, The relation of catastrophic flooding of Mangala Valles, Mars, to faulting of Memnonia Fossae and Tharsis volcanism: Journal of Geophysical Research, v. 95, no. B9, p. 14,315–14,323.

———1992, Kasei Valles, Mars—Interpretation of canyon materials and flood sources: *in* Lunar and Planetary Science Conference, Proceedings, 1992:

Houston, Tex., Lunar and Planetary Institute, v. 22, p. 73–83.

Tanaka, K.L., Chapman, M.G., and Scott, D.H., 1992a, Geologic map of the Elysium region of Mars: U.S. Geological Survey Miscellaneous Investigations Series Map I–2147, scale 1:5,000,000.

Tanaka, K.L., and Golombek, M.P., 1989, Martian tension fractures and the formation of grabens and collapse features at Valles Marineris, *in* Lunar and Planetary Science Conference, Proceedings, 1989: Houston, Tex., Lunar and Planetary Institute, v. 19, p. 383–396.

Tanaka, K.L., Golombek, M.P., and Banerdt, W.B., 1991, Reconciliation of stress and structural histories of the Tharsis region of Mars: Journal of Geophysical Research, v. 96, no. E1, p. 15,617–15,633.

Tanaka, K.L., and Scott, D.H., 1987, Geologic map of the polar regions of Mars: U.S. Geological Survey Miscellaneous Investigations Series Map I–1802–C, scale 1:15,000,000.

Tanaka, K.L., Scott, D.H., and Greeley, Ronald, 1992b, Global stratigraphy, *in* Kieffer, H.H., Jakosky, B.M., Snyder, C.W., and Matthews, M.S., eds., Mars: Tucson, University of Arizona Press, p. 345–382.

Tanaka, K.L., Skinner, J.A., Jr., Hare, T.M., Joyal, Taylor, and Wenker, Alisa, 2003b, Resurfacing history of the northern plains of Mars based on geologic mapping of Mars Global Surveyor data: Journal of Geophysical Research, v. 108, no. E4, p. GDS 24-1 to GDS 24-32 (doc. no: 8043, doi:10.1029/2002JE001908).

Thomson, B.J., and Head, J.W., III, 2001, Utopia Basin, Mars—Characterization of topography and morphology and assessment of the origin and evolution of basin internal structure: Journal of Geophysical Research, v. 106, no. E10, p. 23,209–23,230.

Tsoar, Haim, Greeley, Ronald, and Peterfreund, A.R., 1979, Mars—The north polar sand sea and related wind patterns, Journal of Geophysical Research, v. 84, p. 8167–8182.

Watters, T.R., 1993, Compressional tectonism on Mars: Journal of Geophysical Research, v. 98, no. E9, p. 17,049–17,060.

———2003, Lithospheric flexure and the origin of the dichotomy boundary on Mars: Geology, v. 31, no. 3, p. 271–274.

Wilhelms, D.E., and Squyres, S.W., 1984, The Martian hemispheric dichotomy may be due to a giant impact: Nature, v. 309, p. 138–140.

Wilson, Lionel, and Head, J.W., III, 2002, Tharsis-radial graben systems as the surface manifestations of plume-related dike intrusion complexes—Models and implications, Journal Geophysical Research, v. 107, no. E8, p. 1-1 to 1-24 (doi:10.1029/2001JE001593).

Wise, D.U., Golombek, M.P., and McGill, G.E., 1979, Tectonic evolution of Mars: Journal of Geophysical Research, v. 84, p. 7934–7939.

Witbeck, N.E., Tanaka, K.L., and Scott, D.H., 1991, Geologic map of the Valles Marineris region, Mars: U.S. Geological Survey Miscellaneous Investigations Series Map I–2010, scale 1:5,000,000.

Witbeck, N.E., and Underwood, J.R., Jr., 1984, Geologic map of the Mare Acidalium quadrangle, Mars (revised): U.S. Geological Survey Miscellaneous Investigations Series Map I–1614, scale 1:5,000,000.

Wyatt, M.B., McSween, H.Y., Tanaka, K.L., and Head, J.W., 2004, Global geologic context for surface alteration on Mars: Geology, v. 32, no. 8, p. 645–648.

Zuber, M.T., Solomon, S.C., Phillips, R.J., and 12 others, 2000, Internal structure and early thermal evolution of Mars from Mars Global Surveyor topography and gravity: Science, v. 287, p. 1788–1793.

Table 1. *Descriptions of map units in the northern plains of Mars: areas, crater densities, and superposition relations.*

Unit name	Unit label	Area[1] (10^6 km^2)	N(5)[2]	N(16)[2]	Superposition relations[3]
Amazonis province					
Medusae Fossae unit	AAm	0.90	42.1±6.8	5.5±2.5	<HNn, HBu_1, HBu_2, HAa, AHc, $AHAa_{1s}$, ATl, AEc_3; ~AAa_{2s}; >AEc_1, AEc_3
Amazonis Planitia 2 north unit	AAa_{2n}	0.63	14.3±4.8[4]	---	<HNn, HAa, $AHAa_{1s}$, AAa_{1n}, ATl; ~AAa_{2s}; >AEc_3
Amazonis Planitia 2 south unit	AAa_{2s}	0.45	18.0±6.4[4]	---	<AHc, $AHAa_{1s}$, ATl; ~AAm, AAa_{2n}
Amazonis Planitia 1 north unit	AAa_{1n}	1.37	21.1±3.9	2.9±1.5	<Nn, HNn, HAa, ABv_i, ABv_m; >AAa_{2n}, ATl
Amazonis Planitia 1 south unit	$AHAa_{1s}$	0.60	73.1±11.0	---	<HNn, HAa; >AAa_{2s}, AAa_{2n}, AAm
Arcadia Planitia unit	HAa	1.27	137.4±10.4	21.3±4.1	<Nn, HNn; >AHc, AHEe, $AHAa_{1s}$, AAa_{1n}, AAa_{2n}, ABv_i, ABv_m, $AHAa_{1s}$, AAa_{2s}, AAm, AEc_2, AEc_3
Elysium province					
Cerberus Fossae 3 unit	AEc_3	0.93	31.2±5.8[4]	---	<Nl, Nn, HNn, HBu_1, HBu_2, HAa, AHEe, AEc_1, AEc_2, AAm, AAa_{2n}; <AAm
Cerberus Fossae 2 unit	AEc_2	0.42	81.6±14.0[4]	24.0±7.6	<Nn, HNn, HAa, AHc, AHEe, AEc_1; >AEc_3
Cerberus Fossae 1 unit	AEc_1	0.04	89.7±44.8	---	<AAm; >AEc_2, AEc_3
Tinjar Valles b unit	AEt_b	0.08	---	---	<HBu_2, AHEe, AHc, ABv_i, AEt_a; ~AEt_a
Tinjar Valles a unit	AEt_a	1.32	75.7±7.6[4]	8.3±2.5[4]	<AHc, AHEe, ABv_i, ABv_m; ~AEt_b; ~AEt_b
Elysium rise unit	AHEe	3.47	92.7±5.2	10.7±1.8	<Nn, HNn, HBu_1, HAa, ABv_i; >HBu_2, ABv_m, AEc_2, AEc_3, AEt_a, AEt_b
Tharsis province					
Lycus Sulci unit	ATl	0.41	---	---	<Nn, AAa_{1n}; >AAm, AAa_{2s}, AAa_{2n}
Alba Patera unit	HTa	0.95	76.7±9.0	14.7±3.9	<Nn, HNn; >ABs, ABv_m
Lunae Planum unit	HNTl	0.27	165.5±25.0	41.4±12.5	<Nl, Nn; ~Nn; >HCc_2, HCc_3, AHc
Isidis province					
Isidis Planitia unit	AIi	0.64	59.5±9.7	---	<HNn, HBu_1, HBu_2, HIs; >AHc
Syrtis Major Planum unit	HIs	0.27	120.6±21.0	14.6±7.3	<Nl, Nn, HNn; >AIi
Amenthes Planum unit	HIs	0.04	167.0±63.1	---	<Nl, Nn, HNn; ~HBu_1
Chryse province					
Simud Vallis unit	HCs	0.35	93.9±16.3	28.4±9.0	<Nl, Nn, $HNCc_1$, ~HCc_4; >AHc, AHcf
Chryse Planitia 4 unit	HCc_4	0.34	93.2±16.5	---	<Nl, Nn, $HNCc_1$, HCa, HCc_3; ~HCc_3, HCs; >ABv_m, AHc
Chryse Planitia 3 unit	HCc_3	0.57	86.7±12.4	7.1±3.5	<Nl, Nn, HNTl, $HNCc_1$, HCa, HCc_2; ~HCs, HCc_4; >ABv_m, HCc_4, AHc
Ares Vallis unit	HCa	0.11	52.7±21.5	---	<Nl, Nn, $HNCc_1$, HCc_2; >HCc_3, HCc_4, ABv_m
Chryse Planitia 2 unit	HCc_2	0.49	120.4±15.7	18.4±6.1	<Nl, Nn, $HNCc_1$; >HCc_3, HCc_4, AHc, ABv_m
Chryse Planitia 1 unit	$HNCc_1$	0.43	227.3±23.0	46.4±10.4	<Nl, Nn; >HCc_2, HCc_3, HCc_4, HCs, AHc

Table 1. *Descriptions of map units in the northern plains of Mars: areas, crater densities, and superposition relations—continued*

Unit name	Unit label	Area[1] (10^6 km^2)	N(5)[2]	N(16)[2]	Superposition relations[3]
Borealis province					
Olympia Undae unit	ABo	0.68	---	---	<ABv_i, ABs, ABb_1, ABb_2; >ABb_2
Planum Boreum 2 unit	ABb_2	0.88	---	---	<ABb_1, ABo, ABs, ABv_m, AHc; >ABo
Planum Boreum 1 unit	ABb_1	0.09	---	---	<ABv_i, ABs; >ABb_2, ABo
Astapus Colles unit	ABa	0.24	63.3±16.3[4]	---	<HBu_1, HBu_2, ABv_i, ABv_m
Deuteronilus Mensae 2 unit	ABd_2	0.21	117.0±23.9[4]	---	<Nn, HNn, HBd_1, AHc, ABv_m
Scandia region unit	ABs	1.95	79.2±6.4	10.8±2.4	<ABv_i, ABv_m; >ABb_1, ABb_2, ABo, AHc
Vastitas Borealis marginal unit	ABv_m	2.19	63.0±5.4	7.3±1.8	<Nn, HNn, $HNCc_1$, HBu_1, HBu_2, HBd_1, HCc_2, HAa, AHc, HCc_3, HCc_4, HTa, ~ABv_i; >AHEe, ABs, ABd_2, ABa, AHc, AAa_{1n}, AEt_a
Vastitas Borealis interior unit	ABv_i	15.49	74.5±2.2	7.0±0.7	<Nn, HNn, HBu_1, HBu_2, AHc, AHEe, HCc_2, ~ABv_m; >AHc, ABa, AAa_{1n}, AEt_a, AEt_b, ABb_1, ABb_2, ABs, ABo
Utopia Planitia 2 unit	HBu_2	1.19	91.9±8.8	11.8±3.2	<Nl, Nn, HNn, HBu_1; ~AHEe; >AHc, AHEe, ABv_i, ABv_m, ABa, Aii, AAm, AEt_b, AEc_2, AEc_3
Utopia Planitia 1 unit	HBu_1	1.61	164.9±10.1	22.9±3.8	<Nl, Nn; ~HNn, HIa; >HBu_2, AHc, ABv_i, ABv_m, AHEe, AIi, ABa, AAm, AEc_3
Deuteronilus Mensae 1 unit	HBd_1	0.14	176.1±36.0	51.4±19.4	<Nn; >AHc, ABv_i, ABv_m, ABd_2
Widespread materials					
Crater unit	AHc	2.28	---	---	<Nl, Nn, HNn, HNTl, $HNCc_1$, HBu_1, HBu_2, HTa, HBd_1, HAa, HCc_2, HCc_3, HCc_4, HCs, AHEe, ABv_i, ABv_m, ABs, HIs, AIi, AAm, $AHAa_{1s}$; >AEt_a, AEt_b, AAm, AAa_{2s}, AAa_{2n}, AEc_3, ABb_2, ABd_2
Crater floor unit	AHcf	0.05	---	---	<Nl, Nn, HCs
Nepenthes Mensae unit	HNn	2.80	261.8±9.7	77.9±5.3	<Nl, Nn; ~Nn; >HIa, HBu_1, HBu_2, HBd_1, HTa, HIs, AHEe, AHc, AIi, ABv_i, ABv_m, ABd_2, AEc_2, AEc_3, HAa, $AHAa_{1s}$, AAa_{1n}, AAa_{2n}, AAm
Noachis Terra unit	Nn	3.87	469.3±11.0	144.5±6.1	<Nl; ~Nl, HNn; >HNTl, $HNCc_1$, HBu_1, HBd_1, HIa, HTa, HIs, HCa, HCc_2, HCc_3, HCc_4, HCs, AHEe, AHc, AHcf, ABs, AAa_{1n}, ABd_2, ABv_i, ABv_m, AEc_2, AEc_3, ATl
Libya Montes unit	Nl	1.6546	413.4±15.8	146.9±9.4	~Nn; >Nn, HNn, HNTl, $HNCc_1$, HBu_1, HBu_2, HIa, HIs, HCs, HCa, HCc_2, HCc_3, HCc_4, AHc, HAa, AEc_3

[1] Area includes unit and craters (AHc) occurring within unit.
[2] N(x) = total number of craters >x km in diameter per 10^6 km^2; ---, no data shown where <4 craters counted and for crater units. Crater locations and sizes provided by N.G. Barlow (written commun., 2004).
[3] <, younger than; ~, overlaps in time with; and >, older than.
[4] Crater count includes significant number of embayed or buried craters within unit.